ARMY RESEARCH LABORATORY

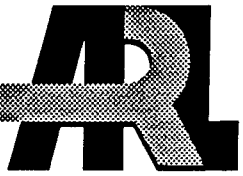

A RASCAL In-Bore Dynamic Analysis of the Task B and Task C Electromagnetic Railguns

Lawrence W. Burton

ARL-TR-726 April 1995

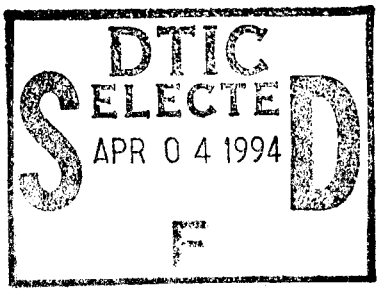

NOTICES

Destroy this report when it is no longer needed. DO NOT return it to the originator.

Additional copies of this report may be obtained from the National Technical Information Service, U.S. Department of Commerce, 5285 Port Royal Road, Springfield, VA 22161.

The findings of this report are not to be construed as an official Department of the Army position, unless so designated by other authorized documents.

The use of trade names or manufacturers' names in this report does not constitute endorsement of any commercial product.

REPORT DOCUMENTATION PAGE

Form Approved
OMB No. 0704-0188

1. AGENCY USE ONLY (Leave blank)	2. REPORT DATE	3. REPORT TYPE AND DATES COVERED
	April 1995	August–September 1994

4. TITLE AND SUBTITLE

A RASCAL In-Bore Dynamic Analysis of the Task B and Task C Electromagnetic Railguns

5. FUNDING NUMBERS

PR: 1L162618AH80

6. AUTHOR(S)

Lawrence W. Burton

7. PERFORMING ORGANIZATION NAME(S) AND ADDRESS(ES)

U.S. Army Research Laboratory
ATTN: AMSRL-WT-PD
Aberdeen Proving Ground, MD 21005-5066

8. PERFORMING ORGANIZATION REPORT NUMBER

ARL-TR-726

9. SPONSORING/MONITORING AGENCY NAME(S) AND ADDRESS(ES)

U.S. Army Armament Research, Development, and Engineering Center
ATTN: SMCAR-FSE
Picatinny Arsenal, NJ 07806-5000

10. SPONSORING/MONITORING AGENCY REPORT NUMBER

11. SUPPLEMENTARY NOTES

12a. DISTRIBUTION/AVAILABILITY STATEMENT

Approved for public release; distribution is unlimited.

12b. DISTRIBUTION CODE

13. ABSTRACT *(Maximum 200 words)*

Previous RASCAL in-bore gun dynamics analyses of 90-mm railguns have shown high transverse accelerations can be expected because of anomalies in the bore straightness. A request was made for similar analyses to be made for the Task B and Task C 90-mm railguns, with the Sabot Launched Electromagnetic Gun KE (SLEKE) II projectile design.

Results of the RASCAL analyses showed the importance of matching the contact stiffness of the rear and front bore riders of the SLEKE II designs. Numerous cases were run to show the effects of variations in contact stiffness. Mismatched contact stiffnesses resulted in elevated transverse accelerations at the less stiff of the two bore riding contacts.

Comparisons of the results of this work are made against previous RASCAL analyses. These results verify the effect a kink in the bore centerline profile has on the projectile's in-bore response.

14. SUBJECT TERMS	15. NUMBER OF PAGES
transverse loadings, electromagnetic railguns, in-bore gun dynamics	68
	16. PRICE CODE

17. SECURITY CLASSIFICATION OF REPORT	18. SECURITY CLASSIFICATION OF THIS PAGE	19. SECURITY CLASSIFICATION OF ABSTRACT	20. LIMITATION OF ABSTRACT
UNCLASSIFIED	UNCLASSIFIED	UNCLASSIFIED	UL

INTENTIONALLY LEFT BLANK.

TABLE OF CONTENTS

		Page
	LIST OF FIGURES	v
	LIST OF TABLES	ix
1.	INTRODUCTION	1
2.	IN-BORE DYNAMICS MODEL	2
2.1	Gun System Models	2
2.2	Barrel Geometry Models	5
2.3	Bore Centerline Profiles	5
2.4	Interior Ballistic Profile	6
2.5	Projectile Geometry	6
3.	RESULTS	10
3.1	Task B Gun	12
3.2	Task C Gun	13
4.	CONCLUSIONS	16
5.	REFERENCES	19
	APPENDIX A: LISTING OF RASCAL INPUT FILES FOR THE TASK B AND TASK C GUNS	21
	APPENDIX B: TRANSVERSE ACCELERATION PLOTS FOR TASK B GUN	29
	APPENDIX C: ANGULAR ACCELERATION PLOTS FOR TASK B GUN	39
	APPENDIX D: TRANSVERSE ACCELERATION PLOTS FOR TASK C GUN	49
	APPENDIX E: ANGULAR ACCELERATION PLOTS FOR TASK C GUN	59
	DISTRIBUTION LIST	69

INTENTIONALLY LEFT BLANK.

LIST OF FIGURES

Figure		Page
1.	Schematic of Task C gun barrel	3
2.	Annular representation of Task C barrel for RASCAL analysis	4
3.	Measured bore centerline profile of the Task B gun	5
4.	Measured bore centerline profile of the Task C gun	6
5.	Interior ballistic load profile of the Task B gun	7
6.	Interior ballistic load profile of the Task C gun	7
7.	SLEKE II projectile configuration	8
8.	Finite element wedge representation of SLEKE II armature	8
9.	Finite element model of quadrilateral block	9
10.	RASCAL geometry model of the SLEKE II projectile	9
11.	Example plot of RASCAL's transverse acceleration prediction	11
12.	Example plot of RASCAL's angular acceleration prediction	11
13.	Rear contact transverse acceleration for case 5 conditions with the Task B gun - rail centerline profile	14
14.	Projectile position vs. time in Task B gun	14
B-1.	Case 1 transverse acceleration from Task B gun - rail centerline	31
B-2.	Case 2 transverse acceleration from Task B gun - rail centerline	31
B-3.	Case 3 transverse acceleration from Task B gun - rail centerline	32
B-4.	Case 4 transverse acceleration from Task B gun - rail centerline	32
B-5.	Case 5 transverse acceleration from Task B gun - rail centerline	32
B-6.	Case 6 transverse acceleration from Task B gun - rail centerline	33
B-7.	Case 7 transverse acceleration from Task B gun - rail centerline	34
B-8.	Case 1 transverse acceleration from Task B gun insulator centerline	34

Figure Page

B-9. Case 2 transverse acceleration from Task B gun insulator centerline 35

B-10. Case 3 transverse acceleration from Task B gun insulator centerline 35

B-11. Case 4 transverse acceleration from Task B gun insulator centerline 36

B-12. Case 5 transverse acceleration from Task B gun insulator centerline 36

B-13. Case 6 transverse acceleration from Task B gun insulator centerline 37

B-14. Case 7 transverse acceleration from Task B gun insulator centerline 37

C-1. Case 1 angular acceleration from Task B gun - rail centerline 41

C-2. Case 2 angular acceleration from Task B gun - rail centerline 41

C-3. Case 3 angular acceleration from Task B gun - rail centerline 42

C-4. Case 4 angular acceleration from Task B gun - rail centerline 42

C-5. Case 5 angular acceleration from Task B gun - rail centerline 43

C-6. Case 6 angular acceleration from Task B gun - rail centerline 43

C-7. Case 7 angular acceleration from Task B gun - rail centerline 44

C-8. Case 1 angular acceleration from Task B gun insulator centerline 44

C-9. Case 2 angular acceleration from Task B gun insulator centerline 45

C-10. Case 3 angular acceleration from Task B gun insulator centerline 45

C-11. Case 4 angular acceleration from Task B gun insulator centerline 46

C-12. Case 5 angular acceleration from Task B gun insulator centerline 46

C-13. Case 6 angular acceleration from Task B gun insulator centerline 47

C-14. Case 7 angular acceleration from Task B gun insulator centerline 47

D-1. Case 1 transverse acceleration from Task C gun - rail centerline 51

D-2. Case 2 transverse acceleration from Task C gun - rail centerline 51

D-3. Case 3 transverse acceleration from Task C gun - rail centerline 52

D-4. Case 4 transverse acceleration from Task C gun - rail centerline 52

Figure		Page
D-5.	Case 5 transverse acceleration from Task C gun - rail centerline	53
D-6.	Case 6 transverse acceleration from Task C gun - rail centerline	53
D-7.	Case 7 transverse acceleration from Task C gun - rail centerline	54
D-8.	Case 1 transverse acceleration from Task C gun insulator centerline	54
D-9.	Case 2 transverse acceleration from Task C gun insulator centerline	55
D-10.	Case 3 transverse acceleration from Task C gun insulator centerline	55
D-11.	Case 4 transverse acceleration from Task C gun insulator centerline	56
D-12.	Case 5 transverse acceleration from Task C gun insulator centerline	56
D-13.	Case 6 transverse acceleration from Task C gun insulator centerline	57
D-14.	Case 7 transverse acceleration from Task C gun insulator centerline	57
E-1.	Case 1 angular acceleration from Task C gun - rail centerline	61
E-2.	Case 2 angular acceleration from Task C gun - rail centerline	61
E-3.	Case 3 angular acceleration from Task C gun - rail centerline	62
E-4.	Case 4 angular acceleration from Task C gun - rail centerline	62
E-5.	Case 5 angular acceleration from Task C gun - rail centerline	63
E-6.	Case 6 angular acceleration from Task C gun - rail centerline	63
E-7.	Case 7 angular acceleration from Task C gun - rail centerline	64
E-8.	Case 1 angular acceleration from Task C gun insulator centerline	64
E-9.	Case 2 angular acceleration from Task C gun insulator centerline	65
E-10.	Case 3 angular acceleration from Task C gun insulator centerline	65
E-11.	Case 4 angular acceleration from Task C gun insulator centerline	66
E-12.	Case 5 angular acceleration from Task C gun insulator centerline	66
E-13.	Case 6 angular acceleration from Task C gun insulator centerline	67
E-14.	Case 7 angular acceleration from Task C gun insulator centerline	67

INTENTIONALLY LEFT BLANK.

LIST OF TABLES

Table		Page
1.	Physical and Material Properties of Task C Barrel	4
2.	Rear and Front Contact Stiffness Values	10
3.	Maximum Projectile Transverse Accelerations Through the Rail Centerline Profile of the Task B Railgun	13
4.	Maximum Projectile Transverse Accelerations Through the Insulator Centerline Profile of the Task B Railgun	13
5.	Maximum Projectile Transverse Accelerations Through the Rail Centerline Profile of the Task C Railgun	15
6.	Maximum Projectile Transverse Accelerations Through the Insulator Centerline Profile of the Task C Railgun	15
7.	Maximum Projectile Transverse Accelerations Through the Rail Centerline Profile of the Task C Railgun With Task B Gun Launch Velocity	16

INTENTIONALLY LEFT BLANK.

1. INTRODUCTION

Electromagnetic (EM) gun projectile designers have spent much time and effort over the past five years to design robust, large caliber, kinetic energy (KE) projectiles. The effort has focused on ensuring structural integrity of the sabot and armature during the in-bore launch cycle. These efforts have paid dividends and resulted in successful launches from 90-mm EM railguns under the auspices of the Sabot Launched Electromagnetic Gun KE (SLEKE) projectile program (Statton, Alexander, and Dethlefsen 1995). While these high-energy test firings have been successful in the sense that a projectile exited the muzzle intact, there has been little experimental effort dedicated to the accuracy issues associated with EM launchers.

Recently, analytical work has been done comparing the in-bore dynamic behavior of projectiles in an EM railgun and a conventional powder cannon (Burton 1993). This work revealed that the bore centerline profiles, typical in state-of-the-art railguns, impart much higher transverse force loading to the projectile than currently found in conventional guns. The calculated lateral acceleration loading in the EM railgun was found to be as much as 10 times that of the conventional gun.

A standard approach used by EM projectile designers is to proof fire their design configurations in conventional powder guns at pressures which produce equivalent maximum axial accelerations and loading rise times as those expected for the intended EM launch. Kaman Sciences Corporation's Rodman cone projectile design was tested in this manner and was successfully launched at the U.S. Army Combat Systems Test Activity (CSTA) at Aberdeen Proving Ground, MD (Statton, Alexander, and Dethlefsen 1995). When this projectile was subsequently launched from the 90-mm railgun at Maxwell Laboratories, there were unexpected in-bore failures.

As a consequence of these failures, an in-bore dynamics analysis was made and it was found that large lateral disturbances were initiated at a "kink" present in the railgun profile (Burton 1995). While this work did not calculate stresses through the projectile body, it did show that high transverse forces were present which were not accounted for in the preliminary finite element (FE) analysis of the design nor present in the conventional gun test firings.

Results of the various in-bore dynamic analysis of EM railguns has highlighted the importance of maintaining a bore centerline profile which does not exhibit large and rapid deviations over the length of

the barrel. Taking centerline measurements has become a standard practice within the EM gun community, and their use with in-bore dynamics models has become more prevalent.

The SLEKE program manager requested that such an in-bore analysis be performed for Kaman Science Corporation's SLEKE II, long-rod, KE projectile design. The investigation was to examine the transverse loading encountered by this projectile when launched from the Task B and Task C 90-mm railguns. This report details this analytical investigation and reports its findings.

2. IN-BORE DYNAMICS MODEL

There are several models and techniques available for modeling the in-bore dynamic interaction between a projectile and gun tube (Hopkins 1990; Rabern and Bannister 1990; Wilkerson 1993). Previous analysis of EM in-bore dynamic response (Burton 1994b) had been made with the Little RASCAL code (Erline and Kregel 1990), which is a quasi-2-dimensional beam element model, and was again the model of choice for this investigation.

The RASCAL dynamics code has five basic input requirements which are as follows: 1) a gun system model, 2) a general barrel geometry configuration, 3) a gun bore centerline profile, 4) an interior ballistic profile, and 5) a projectile geometry description. The specific parameters for both the Task B and Task C railguns are given in the following sections.

2.1 Gun System Models. The Task B railgun is an experimental 90-mm launcher located at the University of Texas Center for Electromechanics (UT-CEM). One of the principal inputs required for the gun system model is the gun stiffness elastic modulus. While this value is readily available for conventional guns with homogeneous cross-sections, calculations are required for the laminated barrel cross-section characteristic of an EM railgun.

Previous work (Burton 1993) determined that the longitudinal elastic modulus of the gun barrel required by the RASCAL model can be calculated for an EM railgun by assuming the barrel to be a composite beam. The resulting equation to calculate the elastic modulus is rewritten here:

$$E_{TOT} I_{TOT} = E_1 I_1 + E_2 I_2 + E_3 I_3 \qquad (1)$$

E_{TOT} represents the effective modulus of the gun barrel for the RASCAL model. I_{TOT} is the gun barrel's moment of inertia. E_1, E_2, and E_3 are the modulus values for each of the material regions that make up the composite gun barrel, while I_1, I_2, and I_3 are the moments of inertia associated with each of these regions. The Task B modulus of 35.4×10^6 psi (2.44×10^5 MPa) has been reported previously (Burton 1993) and was adopted for this study for both the rail and insulator centerline cases.

A schematic of the Task C gun barrel is shown in Figure 1. To simplify the calculations, assumptions were adopted which resulted in the barrel being modeled as a series of nested annuli as shown in Figure 2. This assumption has little affect on the magnitude of the transverse accelerations of interest in this study. Values as small as 25% of the calculated stiffness adopted were used to make calculations with the magnitude of the transverse accelerations differing by only about 1% from those reported here. The dimensions, material moduli, and calculated moments of inertia are given for both the rail and insulator planes in Table 1. Incorporating these values into equation 1 yields an effective longitudinal modulus of 25.3×10^6 psi (1.74×10^5 MPa) in the rail plane and 27.1×10^6 psi (1.87×10^5 MPa) in the insulator plane.

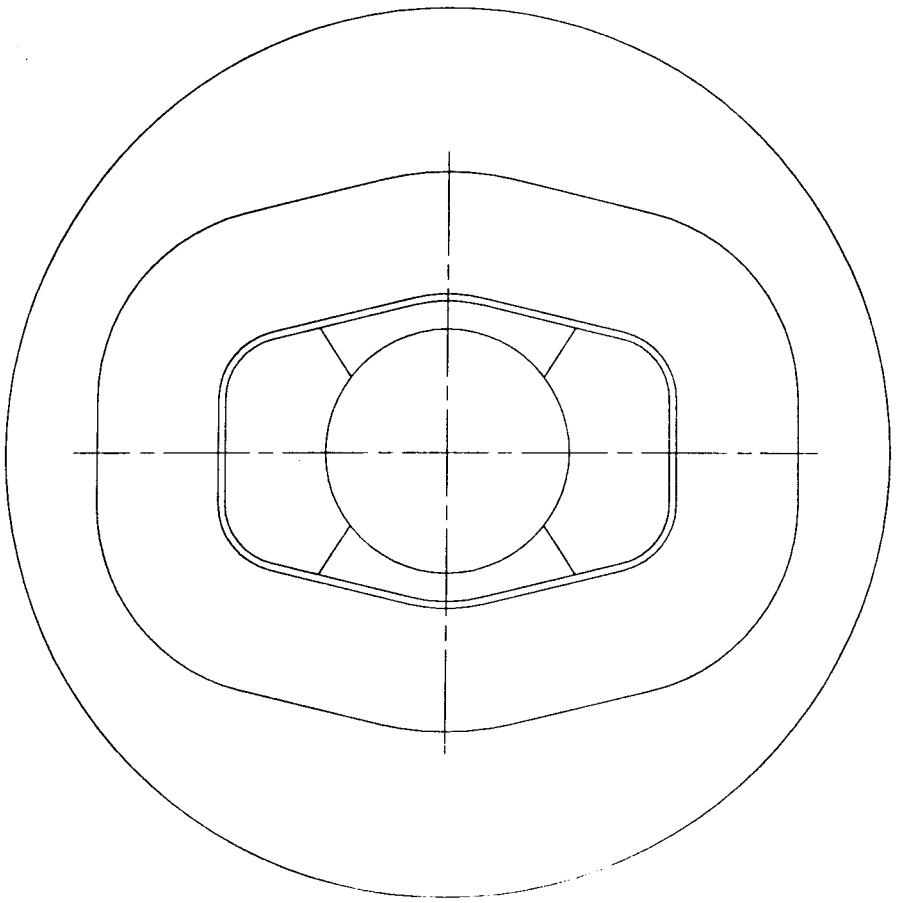

Figure 1. Schematic of Task C gun barrel.

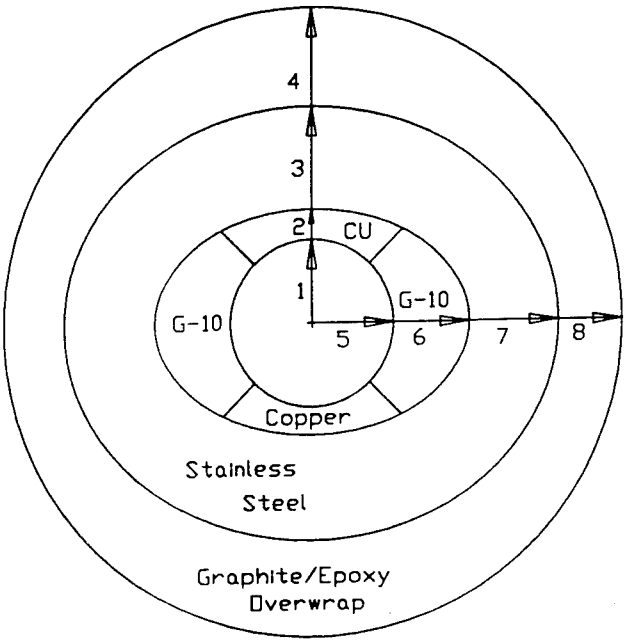

Figure 2. Annular representation of Task C barrel for RASCAL analysis.

Table 1. Physical and Material Properties of Task C Barrel

Radius No.	Radius (in)	Material	Material Modulus (PSI)	Moment of Inertia (in^4)
1	1.77	—(bore)	0	7.74
2	2.25	copper	19×10^6	20.13
3	4.0	stainless steel	27.6×10^6	201.06
4	6.35	graphite/epoxy overwrap	25.0×10^6	1,276.98
5	1.77	—(bore)	0	7.74
6	3.293	G-10 ceramic	44.0×10^6	92.35
7	5.043	stainless steel	27.6×10^6	507.97
8	6.35	graphite/epoxy overwrap	25.0×10^6	1,276.98

The RASCAL data input files used for the Task B and Task C gun system models are given in Appendix A.

2.2 Barrel Geometry Models. Both Task B and Task C guns have nominal bore diameters of 90 mm. From the bore centerline measurements made by CSTA, it was found that the length of the Task C gun, 280 in (7.11 m), is 21% less than the measured length of the Task B gun, 354 in (8.99 m). The RASCAL data input for the barrel geometry models is included in Appendix A.

2.3 Bore Centerline Profiles. Measurements were taken of the bore centerline profiles for both the Task B and Task C guns. The measurement technique was developed by CSTA (Weddle 1986) and has been used extensively to measure conventional powder guns, as well as EM railguns. Basically, the measurements are made by first establishing a line of sight (LOS) from the breech to the muzzle of the barrel. A circular target is then pulled through the barrel with deviations of the target center from the LOS centerline recorded at regular intervals over the entire length of travel.

The measured bore centerline profiles for the Task B and Task C barrels are shown in Figures 3 and 4, respectively. Note that two centerline measurements are required to fully characterize a barrel—in this case, one along the plane of the copper rails and the other along the ceramic insulator plane. The actual measured data values can be seen in Appendix A, where they are compiled in the listing of the RASCAL bore centerline input file. All calculations were made assuming no gravity droop. This is truly representative of the Task B gun which is mounted vertically. Removing gravity from the Task C calculation was done to allow for a direct comparison with the Task B barrel.

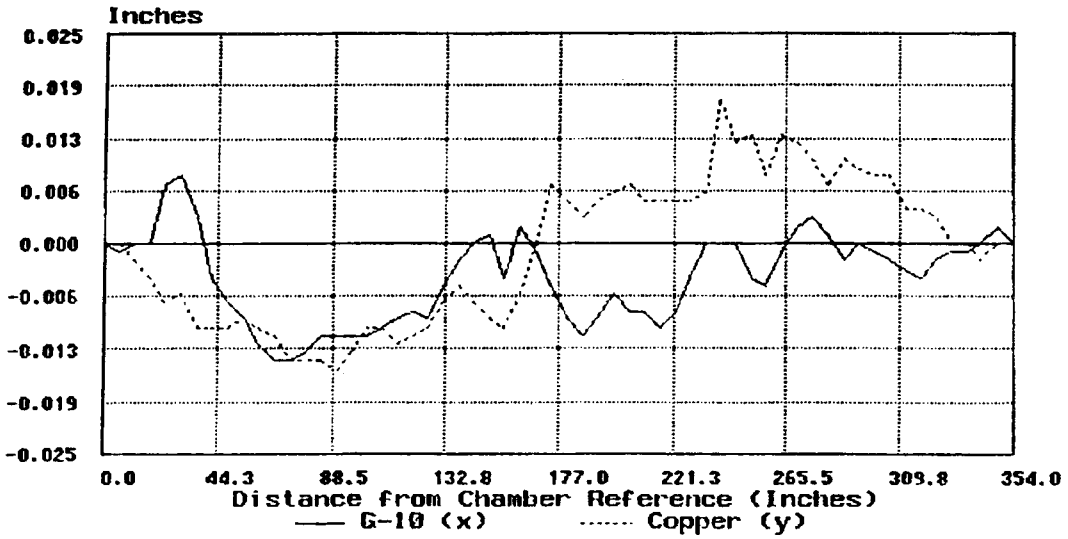

Figure 3. Measured bore centerline profile of the Task B gun.

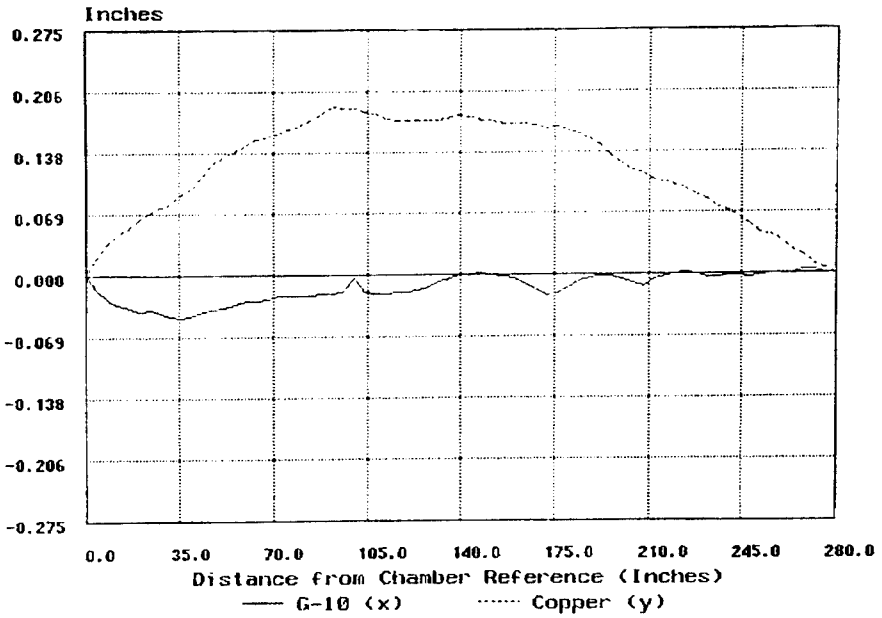

Figure 4. Measured bore centerline profile of the Task C gun.

2.4 Interior Ballistic Profile. The RASCAL code requires a driving force function to simulate the in-bore dynamic motion of the projectile as it travels the length of the barrel. This is accomplished with a velocity vs. time input file. Figure 5 depicts the velocity profile used for the Task B analyses. This profile is a predicted performance based on a UT-CEM simulation. The estimated muzzle velocity is 2,042 m/s (6,700 ft/s). Similar data was also supplied by UT-CEM for the Task C gun and is shown in Figure 6. The Task C gun muzzle velocity was projected to be 1,062 m/s (3,484 ft/s) for a launch of the SLEKE II projectile. The RASCAL input files of the interior ballistic loadings for the two gun systems are listed in Appendix A.

2.5 Projectile Geometry. The RASCAL gun dynamics code was written for axisymmetric, double-ramped sabot, KE rounds. The SLEKE II projectile of interest in this study has a swept-back, nonaxisymmetric, trailing rear armature, as shown by the schematic in Figure 7. Such an armature configuration is somewhat typical of today's KE EM projectiles and requires modifications and assumptions to be made when developing a RASCAL geometry model. One technique used in the past was to ignore the overhanging structure of the armature and use the standard RASCAL geometry modeler incorporated in the code (Burton 1993). This very simple modification does not, however, account for some of the lateral stiffness which the armature trailing arm provides to the projectile structure. A second approach, used previously, bypassed the RASCAL geometry modeler completely. For this method, a projectile was divided into 30 regions or elements of equal length with hand calculations then made for the mass and moment of inertia of each individual element (Burton 1994b). While providing a more accurate representation of the projectile, this technique proved to be a rather labor intensive process.

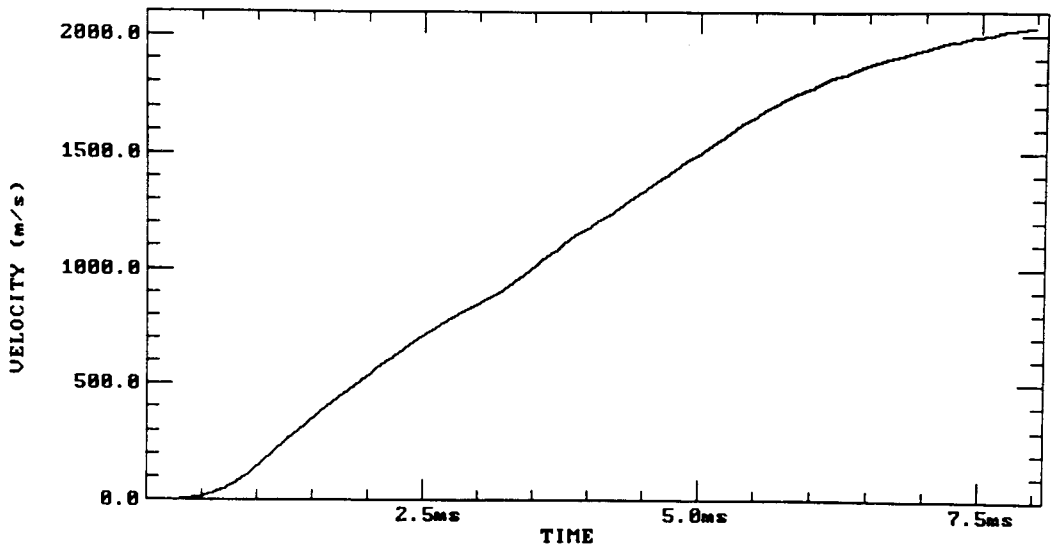

Figure 5. Interior ballistic load profile of the Task B gun.

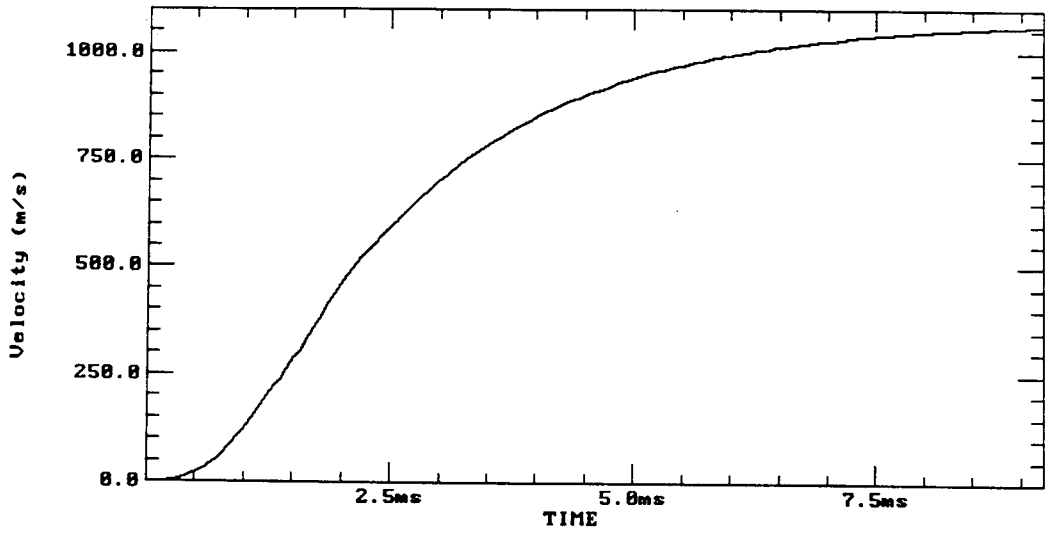

Figure 6. Interior ballistic load profile of the Task C gun.

Therefore, a new method of modeling the armature was incorporated for this study. First, a finite element representation of the overhanging armature was made and is shown as a wedge in Figure 8. A uniform pressure of 1,000 lb (4,448 N) was then placed on the top surface of the wedge, and the displacement of the line halfway up the underside of the wedge was noted. Then a quadrilateral block half the length of the wedge (see Figure 9) was sized such that its deflection under the same uniform

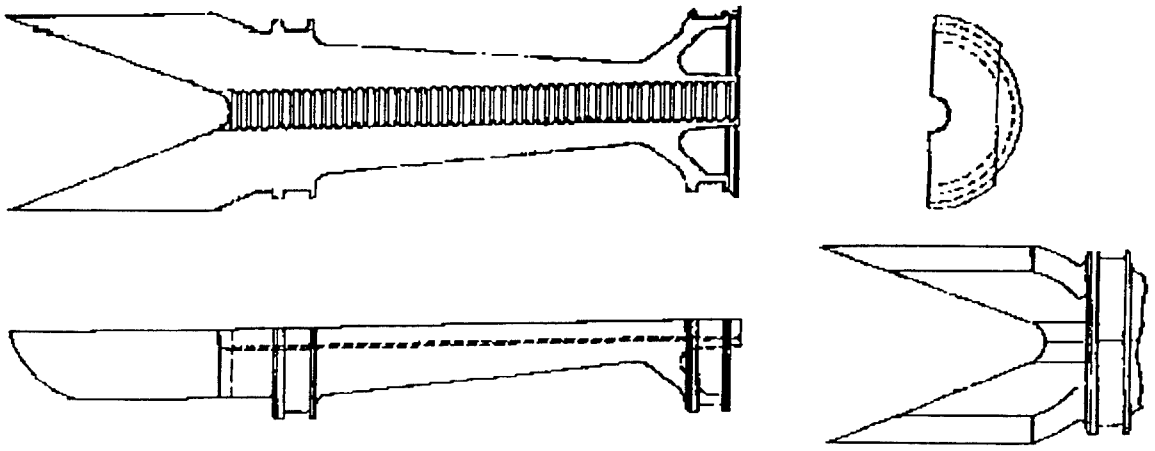

Figure 7. SLEKE II projectile configuration.

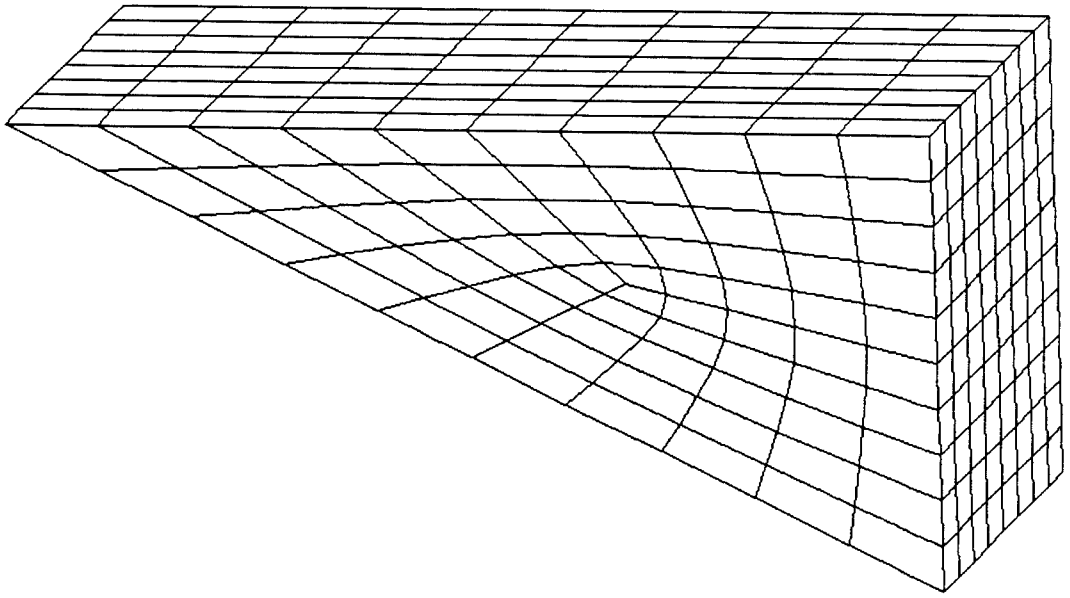

Figure 8. Finite element wedge representation of SLEKE II armature.

1,000-lb load was equal to that of the wedge's midsection. This was an attempt to match the stiffness of the two geometries. The reason for using a block to replace the wedge geometry is that this shape can be represented in RASCAL with no modification to the geometry modeler required. An outline of the

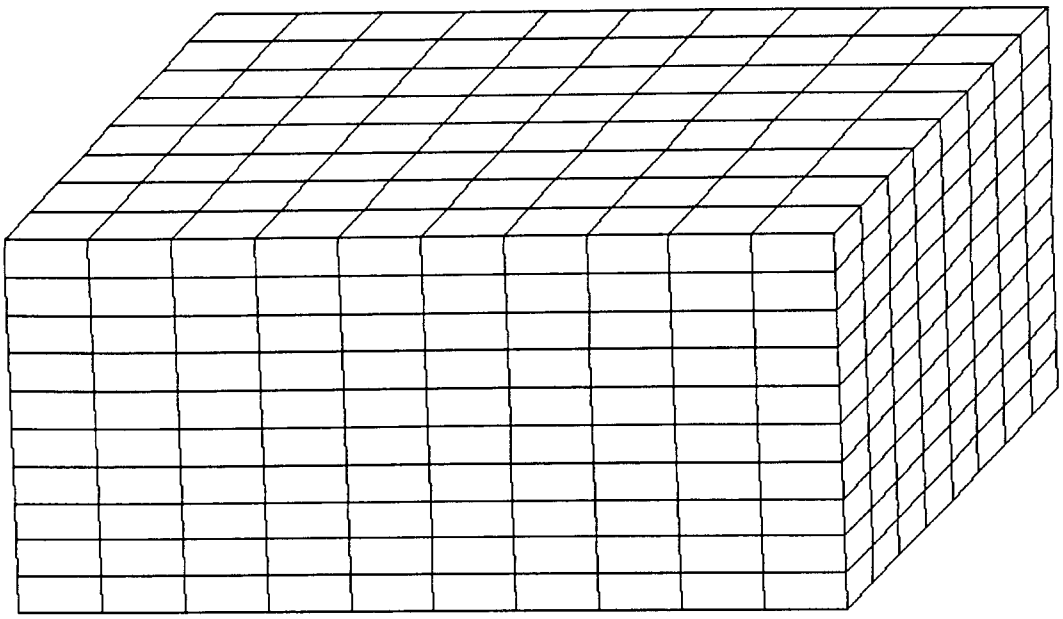

Figure 9. Finite element model of quadrilateral block.

SLEKE II projectile shape for input into RASCAL is shown in Figure 10, with the RASCAL input file provided in Appendix A. A closer approximation could be made by matching the wedge and block displacements at several locations, but at the expense of being a more time-consuming procedure.

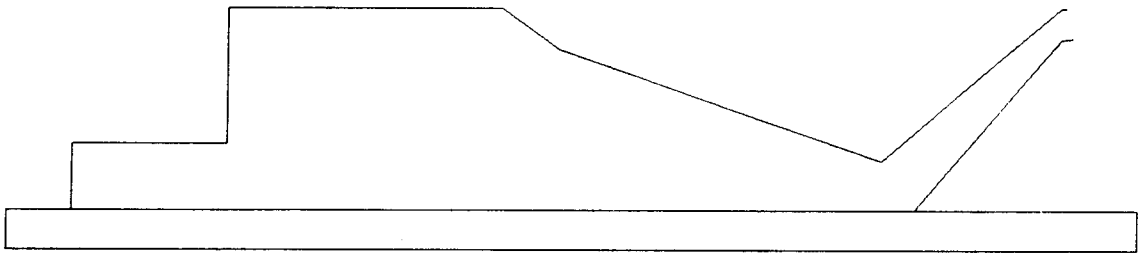

Figure 10. RASCAL geometry model of the SLEKE II projectile.

The other important input parameter for the RASCAL projectile model is the choice of contact stiffness values which greatly influence the dynamic interaction between the projectile and gun barrel (Erline 1991). A variety of combinations were employed for this study and are tabulated in Table 2. The values for cases 1, 2, and 6 were chosen to be consistent with previous analysis done of the Single Shot Gun (SSG) at Green Farm (Burton 1994a). Previous deflection measurements made, as part of the Cannon-Caliber Electromagnetic Gun (CCEMG) program, of an armature with a configuration similar to that of the SLEKE II projectile resulted in a stiffness value of 4.3e06 lb/in (7.53e08 N/m). This value was used for the rear stiffness in cases 3, 4, and 5. The front borerider shape of the SLEKE II is similar to the M829A1 tank round, whose force-deflection measurements had also been made previously (Lyon 1994). The corresponding values for the front contact stiffness of cases 3, 4, and 5 are taken from Lyon's work with the differences in value a consequence of the curve fitting assumptions made for the force vs. deflection data. Case 7 was made part of the investigative matrix to see what effects a more compliant front borerider, in comparison to its rear contact, has on the transverse forces encountered.

Table 2. Rear and Front Contact Stiffness Values

Case No.	Rear Contact Stiffness (lb/in)	Front Contact Stiffness (lb/in)
1	1.0×10^5	1.0×10^5
2	4.3×10^5	4.3×10^5
3	4.3×10^5	6.1×10^5
4	4.3×10^5	8.6×10^5
5	4.3×10^5	1.0×10^6
6	1.0×10^6	1.0×10^6
7	1.0×10^6	4.3×10^5

3. RESULTS

Four sets of RASCAL runs were made using the SLEKE II projectile. The four runs considered the in-bore dynamics of the insulator and rail centerline profiles of both the Task B and Task C guns. The RASCAL output utilized was the beam element velocity data and the angular rate motion of the two contacts. A derivative of time was taken for each value of the beam element velocity data to give a

transverse acceleration of the projectile body. The transverse accelerations at the front and rear contacts and the projectile center of gravity were then extracted. An example plot of the transverse acceleration data is shown in Figure 11. Note that muzzle exit occurs at 8.0 ms so any plotted data beyond that point is extraneous. Similarly, plots of the angular acceleration of the projectile were produced for each case with an example shown in Figure 12.

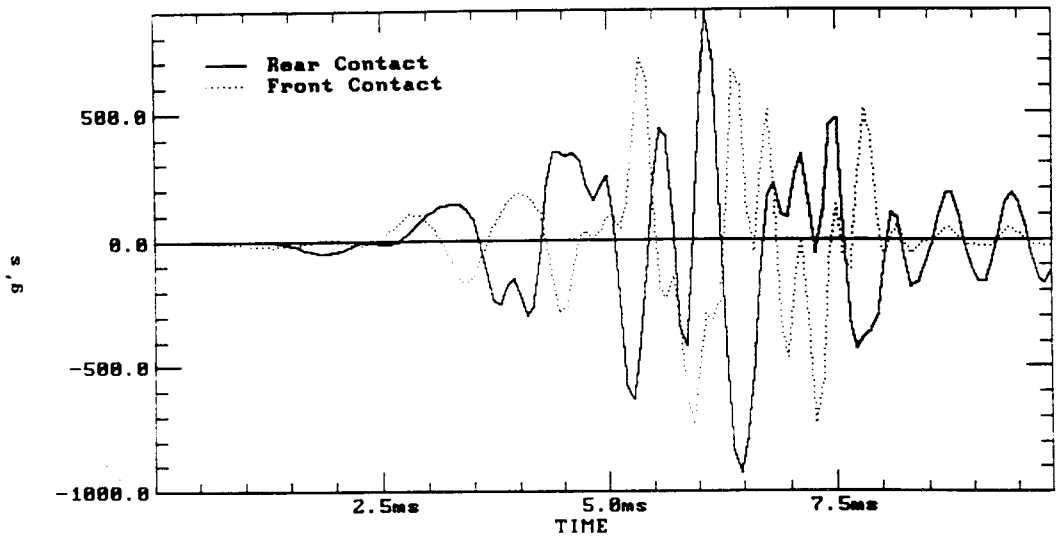

Figure 11. Example plot of RASCAL's transverse acceleration prediction.

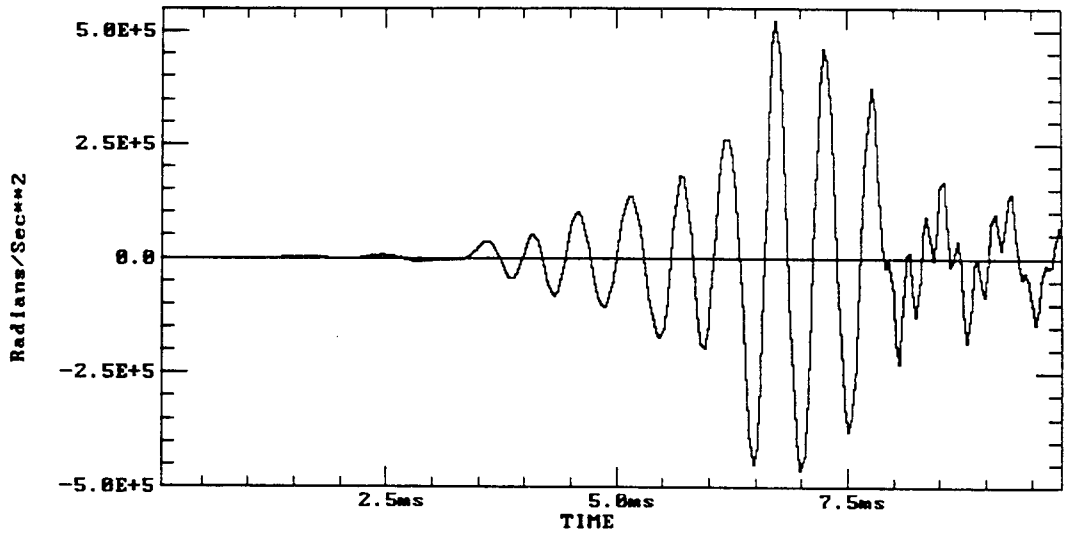

Figure 12. Example plot of RASCAL's angular acceleration prediction.

3.1 Task B Gun. Transverse acceleration plots for the front and rear contacts are given for each of the cases in Appendix B. Likewise, angular acceleration plots of each case are found in Appendix C. For each data run, the maximum transverse acceleration of the front and rear contacts and the projectile center of gravity were found. Tables 3 and 4 list these maximum acceleration values for the Task B rail and insulator profiles, respectively.

A direct comparison with the 90-mm SSG railgun is available for cases 1, 2, and 6 from previous work (Burton 1994a). The transverse accelerations from Task B are reduced by at least 20% from the previous study results. It has been shown previously (Burton 1995) that the centerline profile is the primary driver in determining the magnitude of the transverse acceleration. Thus, although the projectile geometries differ, it is safe to conclude that an improvement in the projectile response of this magnitude is a result of the Task B gun being more benign than the SSG.

Another interesting artifact of the data from the Task B analysis cases is that the importance of stiffness matching at the contacts, for a projectile of this design, is made clear. From Table 3, there are two examples that establish this phenomena. Starting with case 2, which has equal front and rear contact stiffnesses, as the front borerider contact is stiffened, the transverse acceleration at the rear is increased by as much as 60%. The physical explanation resides primarily in the design of the SLEKE II projectile which has its bore contacts at the ends of the projectile, away from the projectile center of gravity. Thus, as a contact is stiffened (in cases 2–5, the front), we are in effect clamping the projectile more tightly in place at one end which produces a cantilever vibrational effect. As transverse forces are imparted to the projectile, the clamped front end remains relatively fixed while the rear fishtails. We see this phenomena again in going from case 6 to case 7, where, as the front contact stiffness is reduced, this newly "unclamped" end has a 68% increase in transverse acceleration.

Figure 13 shows a plot of the rear contact transverse acceleration for case 5. Note that the high transverse accelerations are initiated just after 5.0 ms. This is representative of the other Task B gun transverse acceleration plots, which are provided in Appendix B. By integrating the Task B velocity vs. time curve in Figure 5, the projectile in-bore position as a function of time is obtained and is plotted in Figure 14. This plot shows that after 5.0 ms the projectile has traveled a little more than 4.0 m (157 in). A look back at the Task B centerline profiles in Figure 3 shows this location, 157 in, to be in the region of a kink in both the rails and insulators. The problems associated with kinked rail centerlines have been presented before (Burton 1995), and this provides further evidence supporting the importance of a relatively straight bore profile.

Table 3. Maximum Projectile Transverse Accelerations Through the Rail Centerline Profile of the Task B Railgun

Case No.	Maximum Transverse Acceleration (g's)		
	Rear Contact	Center of Gravity	Front Contact
1	927	553	736
2	7,706	3,224	5,451
3	10,295	4,621	5,524
4	12,325	5,857	7,302
5	11,959	6,337	8,111
6	7,617	3,436	4,959
7	7,680	3,585	8,308

Table 4. Maximum Projectile Transverse Accelerations Through the Insulator Centerline Profile of the Task B Railgun

Case No.	Maximum Transverse Acceleration (g's)		
	Rear Contact	Center of Gravity	Front Contact
1	2,038	904	1,180
2	4,835	2,379	3,487
3	7,105	2,811	3,583
4	11,113	4,825	5,113
5	12,838	5,866	6,388
6	9,230	3,771	7,396
7	9,182	2,732	10,010

3.2 Task C Gun. Like the Task B gun analysis, the Task C cases extracted plots of the transverse and angular accelerations which are given for the front and rear contacts of each case in Appendices D and E, respectively. The maximum transverse acceleration values for the rail and insulator centerline profiles are given in Tables 5 and 6, respectively.

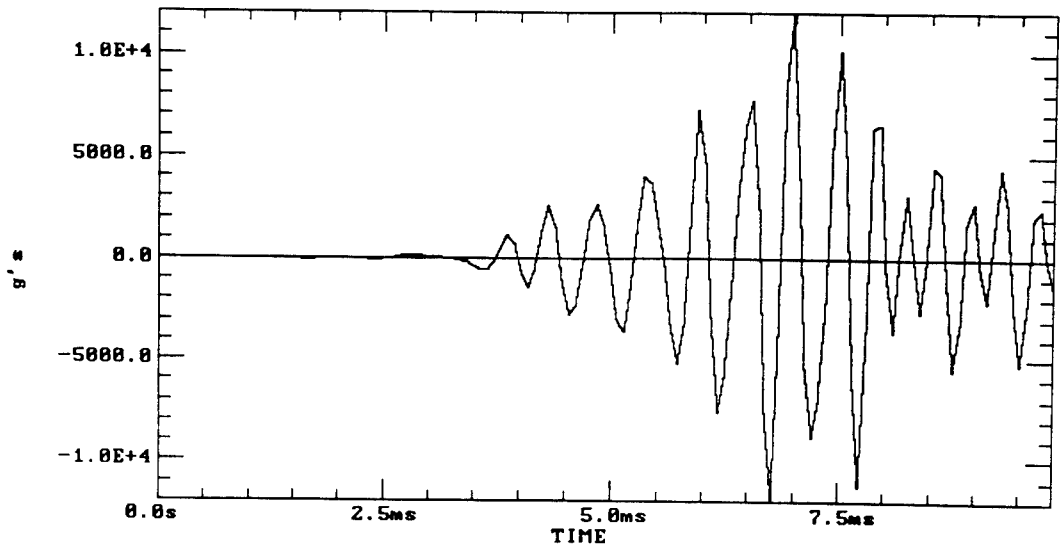

Figure 13. Rear contact transverse acceleration for case 5 conditions with the Task B gun - rail centerline profile.

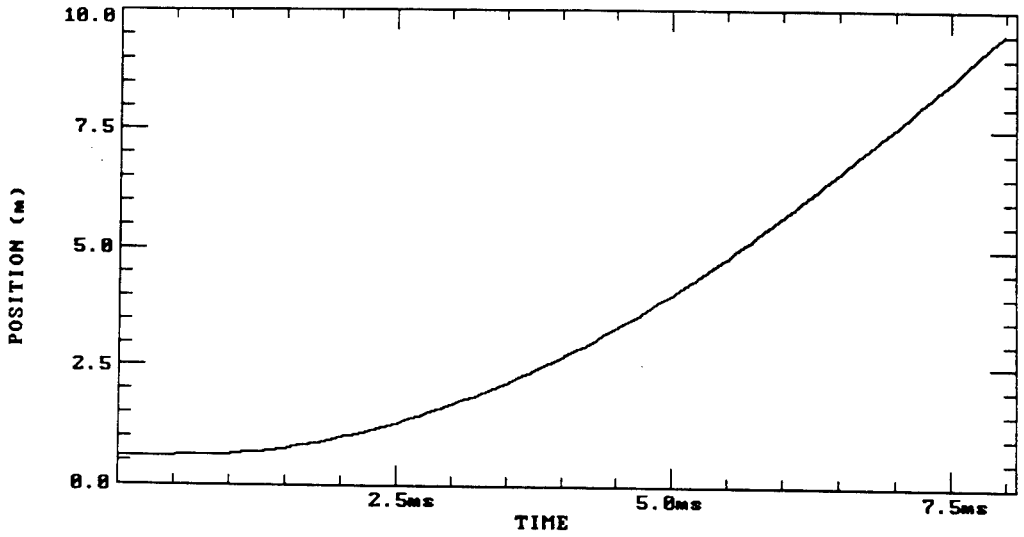

Figure 14. Projectile position vs. time in Task B gun.

The most obvious result from these tables is the insulator cases exhibit much greater transverse accelerations than those of the rails. This can be especially confusing if one refers back to the Task C centerline profiles in Figure 6, which shows that the rail centerline is displaced much more than that of the insulator. Intuitively, one would expect the more displaced centerline to result in a more aggravated response. The fact that the opposite is true relates back to the kinked tube phenomena touched on above. High lateral loads are imparted to the projectile when it must traverse a relatively small radius of curvature, such as found with a kink, which has a large deviation from the line of travel over a very short distance. For the rail profile, the projectile must travel a course with a large deviation from the true centerline, but this is done over the entire length of the barrel, thus minimizing the radius of curvature.

Table 5. Maximum Projectile Transverse Accelerations Through the Rail Centerline Profile of the Task C Railgun

Case No.	Maximum Transverse Acceleration (g's)		
	Rear Contact	Center of Gravity	Front Contact
1	1,867	929	1,606
2	2,870	2,770	4,001
3	3,119	3,206	2,207
4	3,201	3,463	2,707
5	3,235	3,233	1,830
6	1,762	4,406	1,692
7	1,931	3,509	4,270

Table 6. Maximum Projectile Transverse Accelerations Through the Insulator Centerline Profile of the Task C Railgun

Case No.	Maximum Transverse Acceleration (g's)		
	Rear Contact	Center of Gravity	Front Contact
1	2,296	934	2,241
2	8,362	4,306	11,020
3	10,438	5,140	6,716
4	12,139	6,586	5,904
5	12,004	6,888	6,914
6	5,040	4,618	4,437
7	4,837	4,850	9,680

The other noticeable result from Table 5 is the exceptionally low values of the transverse accelerations. These values are well below all the other Task B and Task C cases presented in this report, as well as those values reported for previous EM RASCAL in-bore dynamics studies. To unravel this dilemma, it

was noted that the interior ballistic model used for the Task C gun had a relatively low muzzle velocity of 1,062 m/s. It was believed this low velocity may be the cause of the reduced acceleration values. To test this postulate, two more RASCAL runs were made. These runs took the case 2 and case 4 conditions, but used the higher velocity forcing function of the Task B gun. Table 7 lists the maximum acceleration values for these two cases.

Table 7. Maximum Projectile Transverse Accelerations Through the Rail Centerline Profile of the Task C Railgun With Task B Gun Launch Velocity

Stiffness Value (lb/in)		Maximum Transverse Acceleration (g's)		
Rear	Front	Rear Contact	Center of Gravity	Front Contact
4.3×10^5	4.3×10^5	5,259	3,276	5,357
4.3×10^5	8.6×10^5	10,269	5,736	8,179

The resulting values indeed show that the low velocity used in the Task C simulation was responsible for the much reduced transverse acceleration values. While the Task C barrel exhibits transverse accelerations less than the Task B gun at a comparable velocity, the magnitudes are relatively equivalent. Unfortunately, this also means the accelerations induced by the insulator profile, reported in Table 6, are probably well below those which would occur at higher velocities, and will likely exceed those found for the Task B barrel.

4. CONCLUSIONS

The results of the RASCAL in-bore dynamic analysis of the Task B and Task C 90-mm railguns point out an important consideration for EM projectile designers. Namely, when adopting a saddle sabot arrangement (that is, one with boreriding contacts at the ends of the projectile away from the projectile center of gravity), it is important to match the relative stiffness of the front and rear contacts. This investigation found that as the difference between the front and rear contact stiffness is increased, the resulting transverse accelerations are also elevated. Another means of avoiding this problem is to adopt a mid-riding armature configuration, thus resulting in a shape very near that of double-ramped KE projectiles which are the current standard.

Comparisons of the results from the Task B gun with those obtained in a previous RASCAL analysis of the SSG at Green Farms show the Task B gun to have the less severe centerline. The initial comparison of the Task B and Task C rail centerline profiles appears to favor the Task B system. However, much of the advantage results from the large difference in the velocity regimes employed in the analysis. Under equivalent loadings, the Task B and C rail centerline profiles produce approximately the same magnitude of transverse acceleration. The insulator profile of the Task C gun likely induces higher transverse accelerations than are present in the Task B barrel under equivalent velocity loading conditions.

As with previous RASCAL analyses of EM gun systems, the modeling of the trailing armature required a nonstandard technique. For this investigation the wedge shape of the armature was replaced with a block which had equivalent displacements under a uniform load along a single line in both structures. A more exact representation could be acquired by matching the deflected shapes of the wedge and block at numerous locations and would likely result in a more precise determination of the lateral loading.

INTENTIONALLY LEFT BLANK.

5. REFERENCES

Burton, L. "A Comparison of In-Bore Projectile Motion From an Electromagnetic Railgun vs. that of a Conventional Cannon Barrel." ARL-TR-295, U.S. Army Research Laboratory, Aberdeen Proving Ground, MD, October 1993.

Burton, L. "Effects of Bore Profile on EM-Launched Projectiles." 19th Army Science Conference, Orlando, FL, June 20–23, 1994a.

Burton, L. "In-Bore Dynamic Response Analysis of a SLEKE I Projectile Fired From the Single Shot Gun (SSG) Railgun." ARL-TR-470, U.S. Army Research Laboratory, Aberdeen Proving Ground, MD, July 1994b.

Burton, L. "Implications of Rail Straightness for EM-Launched Projectiles." IEEE Transactions on Magnetics, vol. 31, no. 1, pp. 101–106, January 1995.

Erline, T. F. "Projectile Spring Constants Significance to Modeling With the Little RASCAL Gun Dynamics Program." BRL-TR-3224, U.S. Army Ballistic Research Laboratory, Aberdeen Proving Ground, MD, April 1991.

Erline, T. F., and M. D. Kregel. "Flexible Projectile Modeling Using the Little RASCAL Gun Dynamics Program." Proceedings of the Sixth U.S. Army Symposium on Gun Dynamics, Tamiment, PA, May 1990.

Hopkins, D. A. "Modeling Gun Dynamics With Three-Dimensional Beam Elements." Proceedings of the Sixth U.S. Army Symposium on Gun Dynamics, Tamiment, PA, May 1990.

Lyon, D. H. "Radial Stiffness Measurements of 120-mm Tank Projectiles." ARL-TR-392, U.S. Army Research Laboratory, Aberdeen Proving Ground, MD, April 1994.

Rabern, D. A., and K. A. Bannister. "Finite Element Models to Predict the Structural Response of 120-mm Sabot/Rods During Launch." Proceedings of the Sixth U.S. Army Symposium on Gun Dynamics, Tamiment, PA, May 1990.

Statton, E. S., A. Alexander, and R. Dethlefsen. "Firings of Tactically-Successful Air-Defense Projectiles From a 90mm Electromagnetic Rail Gun." IEEE Transactions on Magnetics, vol. 31, no. 1, pp. 248–252, January 1995.

Weddle, A. L. "Methodology Investigation of Gun-Tube Straightness Measurements." USACSTA-6439, Combat Systems Testing Activity, Aberdeen Proving Ground, MD, October 1986.

Wilkerson, S. A. "The Use of Structural Codes to Study Gun Dynamics." ARL-TR-49, U.S. Army Research Laboratory, Aberdeen Proving Ground, MD, February 1993.

INTENTIONALLY LEFT BLANK.

APPENDIX A:

LISTING OF RASCAL INPUT FILES FOR THE TASK B AND TASK C GUNS

INTENTIONALLY LEFT BLANK.

RASCAL File Listing of the Task B Gun Centerline Measurement

2	E	
	insulator	rail
axial	<- +>	v- +^
0.0	0.000	0.000
6.0	0.002	0.000
13.0	0.000	-0.002
18.0	-0.001	0.000
24.0	-0.001	0.000
30.0	-0.002	0.003
36.0	-0.004	0.004
42.0	-0.003	0.004
48.0	-0.002	0.008
54.0	-0.001	0.008
60.0	0.000	0.009
66.0	-0.002	0.010
72.0	0.001	0.007
78.0	0.003	0.010
84.0	0.002	0.012
90.0	-0.001	0.013
96.0	-0.005	0.008
102.0	-0.004	0.013
108.0	0.000	0.012
114.0	0.000	0.017
120.0	0.000	0.006
126.0	0.004	0.005
132.0	-0.008	0.005
138.0	-0.010	0.005
144.0	-0.008	0.005
150.0	-0.008	0.007
156.0	-0.006	0.006
162.0	-0.009	0.005
168.0	-0.011	0.003
174.0	-0.009	0.005
180.0	-0.005	0.007
186.0	-0.001	0.000
192.0	0.002	-0.006
198.0	-0.004	-0.010
204.0	0.001	-0.009
210.0	0.000	-0.007
216.0	-0.002	-0.005
222.0	-0.005	-0.007
228.0	-0.009	-0.010
234.0	-0.008	-0.011
240.0	-0.009	-0.012
246.0	-0.010	-0.010
252.0	-0.011	-0.010
258.0	-0.011	-0.013
264.0	-0.011	-0.015
270.0	-0.011	-0.014
276.0	-0.013	-0.014
282.0	-0.014	-0.014
288.0	-0.014	-0.011
294.0	-0.012	-0.010
300.0	-0.009	-0.009
306.0	-0.007	-0.010
312.0	-0.004	-0.010
318.0	0.003	-0.010
324.0	0.008	-0.006
330.0	0.007	-0.007
336.0	0.000	-0.004
342.0	0.000	-0.002
348.0	-0.001	0.000
354.0	0.000	0.000

RASCAL File Listing of the Task B Gun Velocity Vs. Time Prediction

3 m 2 1.0

time (ms)	velocity (m/s)	position (m)	time (ms)	velocity (m/s)	position (m)
0.000	0.112555E-13	0.609600	4.200	1237.79	2.93991
0.100	0.112555E-13	0.609600	4.300	1266.17	3.06510
0.200	0.312483	0.609606	4.400	1297.75	3.19328
0.300	2.82988	0.609740	4.500	1333.62	3.32482
0.400	7.87869	0.610264	4.600	1369.42	3.45998
0.500	14.9248	0.611360	4.700	1402.89	3.59951
0.600	28.6949	0.613487	4.800	1435.10	3.74137
0.700	48.1299	0.617297	4.900	1465.40	3.88649
0.800	70.4943	0.623168	5.000	1494.47	4.03448
0.900	102.984	0.631768	5.100	1525.45	4.18546
1.000	143.647	0.644047	5.200	1559.18	4.33967
1.100	186.096	0.660539	5.300	1592.70	4.49728
1.200	227.957	0.681314	5.400	1624.26	4.65823
1.300	269.198	0.706171	5.500	1654.09	4.82210
1.400	309.773	0.735122	5.600	1682.25	4.98879
1.500	349.644	0.768100	5.700	1708.77	5.15825
1.600	388.775	0.805027	5.800	1733.76	5.33029
1.700	427.135	0.845829	5.900	1757.31	5.50477
1.800	464.702	0.890424	6.000	1779.49	5.68155
1.900	501.453	0.938733	6.100	1800.40	5.86049
2.000	537.359	0.990677	6.200	1820.12	6.04146
2.100	572.423	1.04616	6.300	1838.71	6.22435
2.200	606.617	1.10512	6.400	1856.26	6.40902
2.300	639.933	1.16745	6.500	1872.80	6.59542
2.400	672.375	1.23306	6.600	1888.39	6.78346
2.500	703.927	1.30188	6.700	1903.11	6.97303
2.600	734.604	1.37381	6.800	1917.01	7.16404
2.700	764.398	1.44877	6.900	1930.13	7.35641
2.800	793.313	1.52666	7.000	1942.53	7.55005
2.900	821.366	1.60740	7.100	1954.26	7.74490
3.000	848.558	1.69091	7.200	1965.35	7.94089
3.100	874.889	1.77713	7.300	1975.84	8.13797
3.200	900.310	1.86592	7.400	1985.77	8.33607
3.300	929.905	1.95739	7.500	1995.17	8.53513
3.400	965.535	2.05211	7.600	2004.07	8.73511
3.500	1004.87	2.15064	7.700	2012.51	8.93595
3.600	1042.65	2.25306	7.800	2020.51	9.13761
3.700	1078.89	2.35914	7.900	2028.09	9.34005
3.800	1113.60	2.46876	8.000	2035.28	9.54322
3.900	1146.82	2.58180	8.100	2042.11	9.74710
4.000	1178.60	2.69809			
4.100	1208.98	2.81749			

RASCAL File Listing of Task B Gun Description

```
1  m
Gun Description File of Task B Gun
0.0        5.0e7
1.3188     5.0e7
2.5e-05
675.0     0.559
0.148     0.273
0.298     0.0     0.0
0.0460    0.045
0.3048    0.4826
0.0       2.46e10 5342.2     2.46e10     5342.2
```

RASCAL File Listing of Task B Gun Barrel Description

```
1  E
UT-CEM Task B Barrel Description
0.0      9.0
155.0    9.0
354.0    9.0
```

RASCAL File Listing of SLEKE II Projectile Description

```
1  E
SLEKE II projectile
4.3e05     6.1e05
6
0.803       0.844
2.702       0.844
2.703       1.773
4.721       1.773
5.5322      1.1705
10.737      0.763
     0.95      12.096
4
10.737      0.763     0.325
11.571      1.263     0.773
11.696      1.775     1.023
12.496      1.775     1.4675
12.83     0.325      1.3      2.73
0.001
51.0e06     0.64
10.0e06     0.1
51.0e06     0.64
10.0e06     0.1
```

RASCAL File Listing of Task C Gun Description

```
1  m
Gun Description File of Task C Gun
0.0        5.0e7
1.3188     5.0e7
2.5e-05
675.0     0.559
0.148     0.273
0.298     0.0     0.0
0.0460    0.045
0.3048    0.4826
0.0      1.74e11(rails); 1.87e11(ins) 3792.2  1.47e11(rails; 1.87e11(ins) 3792.2
```

RASCAL File Listing of Task C Gun Barrel Description

```
1  E
Task C Barrel Description
0.0      12.7
155.0    12.7
280.0    12.7
```

RASCAL File Listing of Task C Gun Centerline Measurement

```
  2      E
              insulator        rail                              insulator        rail
axial          v-  +^          <-  +>          axial              v-  +^          <-  +>
  0.0          0.000           0.000           144.0              -0.004          0.178
  4.0          0.001           0.007           148.0              -0.009          0.176
  8.0          0.005           0.010           152.0              -0.014          0.175
 12.0          0.005           0.022           156.0              -0.017          0.175
 16.0          0.001           0.027           160.0              -0.019          0.176
 20.0          0.001           0.036           164.0              -0.020          0.176
 24.0          0.000           0.045           168.0              -0.021          0.177
 28.0         -0.002           0.047           172.0              -0.021          0.182
 32.0         -0.004           0.056           176.0              -0.019          0.185
 36.0         -0.002           0.063           180.0              -0.004          0.188
 40.0         -0.003           0.072           184.0              -0.019          0.188
 44.0         -0.005           0.076           188.0              -0.021          0.189
 48.0         -0.004           0.084           192.0              -0.022          0.182
 52.0          0.000           0.089           196.0              -0.024          0.174
 56.0          0.003           0.096           200.0              -0.024          0.169
 60.0          0.000           0.100           204.0              -0.024          0.165
 64.0         -0.003           0.104           208.0              -0.024          0.159
 68.0         -0.006           0.106           212.0              -0.027          0.158
 72.0         -0.014           0.113           216.0              -0.029          0.153
 76.0         -0.010           0.118           220.0              -0.030          0.147
 80.0         -0.006           0.125           224.0              -0.033          0.141
 84.0         -0.002           0.135           228.0              -0.037          0.133
 88.0         -0.002           0.146           232.0              -0.039          0.127
 92.0         -0.005           0.154           236.0              -0.040          0.113
 96.0         -0.009           0.160           240.0              -0.045          0.100
100.0         -0.015           0.164           244.0              -0.048          0.093
104.0         -0.022           0.166           248.0              -0.047          0.081
108.0         -0.023           0.165           252.0              -0.042          0.077
112.0         -0.016           0.169           256.0              -0.039          0.071
116.0         -0.010           0.171           260.0              -0.040          0.063
120.0         -0.005           0.171           264.0              -0.036          0.054
124.0         -0.003           0.171           268.0              -0.033          0.047
128.0          0.001           0.174           272.0              -0.027          0.036
132.0          0.003           0.174           276.0              -0.015          0.020
136.0          0.000           0.179           280.0               0.000          0.000
140.0         -0.001           0.180
```

RASCAL File Listing of Task C Gun Velocity Vs. Time Projection

```
2  m  2  1.0
time        velocity
(ms)         (m/s)
0.000         0.0
0.098245      0.0
0.196489      1.0
0.294734      5.0
0.392978     12.0
0.491223     20.0
0.589468     32.0
0.687713     47.0
0.785957     68.0
0.884202     92.0
0.982446    120.0
1.0807      149.0
1.1789      181.0
1.2772      216.0
1.3754      239.0
1.4737      280.0
1.5719      304.0
1.6702      344.0
1.7684      382.0
1.8666      418.0
1.9649      451.0
2.0631      483.0
2.1614      512.0
2.2596      540.0
2.3579      559.0
2.4561      584.0
2.5544      607.0
2.6526      630.0
2.7509      651.0
2.8491      672.0
2.9473      692.0
3.0456      710.0
3.1438      728.0
3.2421      745.0
3.3403      761.0
3.4386      776.0
3.5368      790.0
3.6351      804.0
3.7333      817.0
3.8315      830.0
3.9298      842.0
4.0280      853.0
4.1263      864.0
4.2245      874.0
4.3228      884.0
4.4210      893.0
4.5193      902.0
```

```
time        velocity
(ms)         (m/s)
4.6175      910.0
4.7157      918.0
4.8140      926.0
4.9122      933.0
5.0105      940.0
5.1087      947.0
5.2070      953.0
5.3052      959.0
5.4035      964.0
5.5017      970.0
5.5999      975.0
5.6982      980.0
5.7964      985.0
5.8947      989.0
5.9929      993.0
6.0911      997.0
6.1894     1001.0
6.2977     1005.0
6.3859     1008.0
6.4841     1012.0
6.5824     1015.0
6.6806     1018.0
6.7789     1021.0
6.8771     1024.0
6.9754     1026.0
7.0736     1029.0
7.1719     1031.0
7.2701     1033.0
7.3684     1036.0
7.4666     1038.0
7.5648     1040.0
7.6631     1042.0
7.7613     1043.0
7.8596     1045.0
7.9578     1047.0
8.0561     1048.0
8.1543     1050.0
8.2526     1051.0
8.3508     1053.0
8.4490     1054.0
8.5473     1055.0
8.6455     1056.0
8.7438     1057.0
8.8420     1058.0
8.9403     1059.0
9.0385     1060.0
9.1368     1061.0
9.2350     1062.0
```

INTENTIONALLY LEFT BLANK.

APPENDIX B:

TRANSVERSE ACCELERATION PLOTS FOR TASK B GUN

INTENTIONALLY LEFT BLANK.

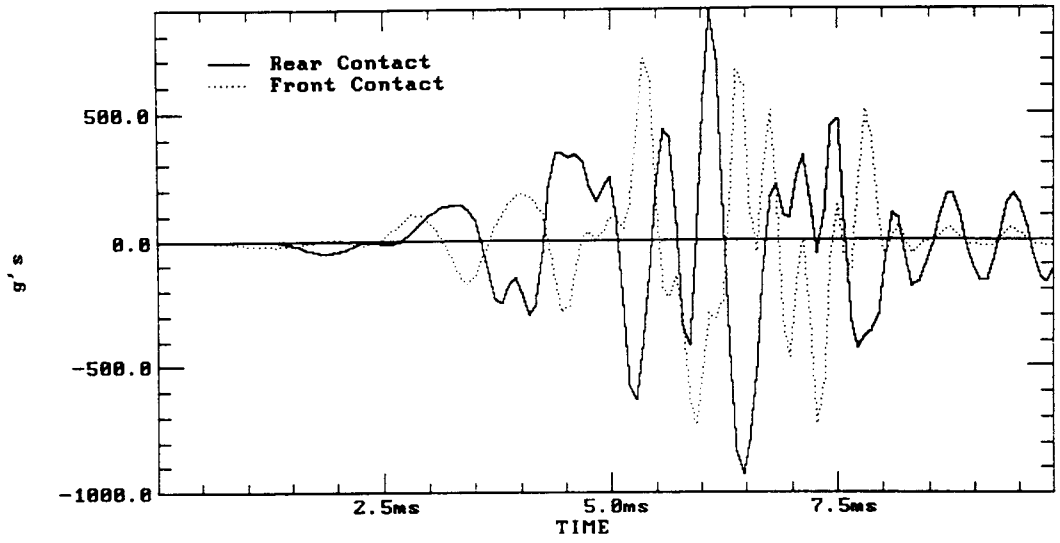

Figure B-1. Case 1 transverse acceleration from Task B gun - rail centerline.

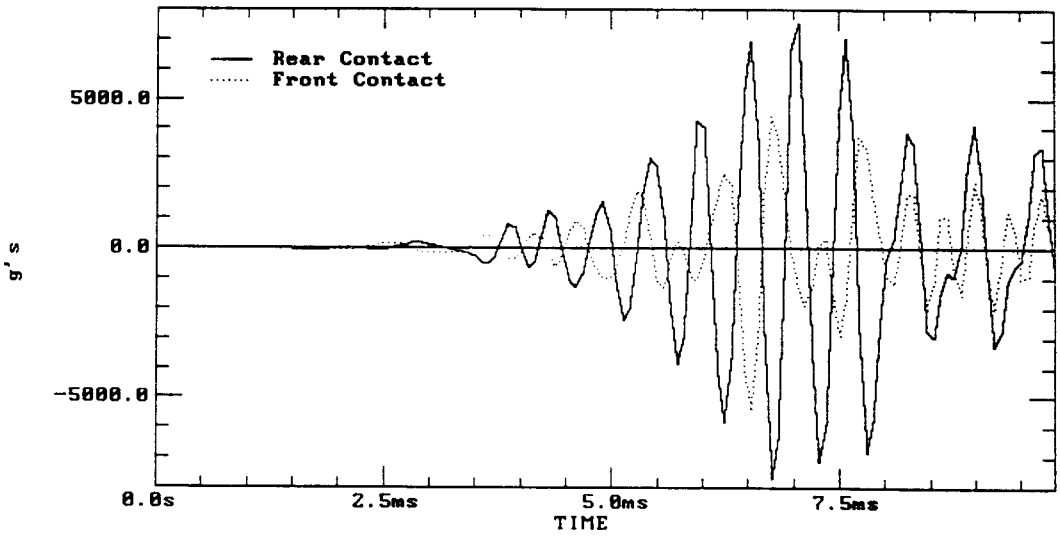

Figure B-2. Case 2 transverse acceleration from Task B gun - rail centerline.

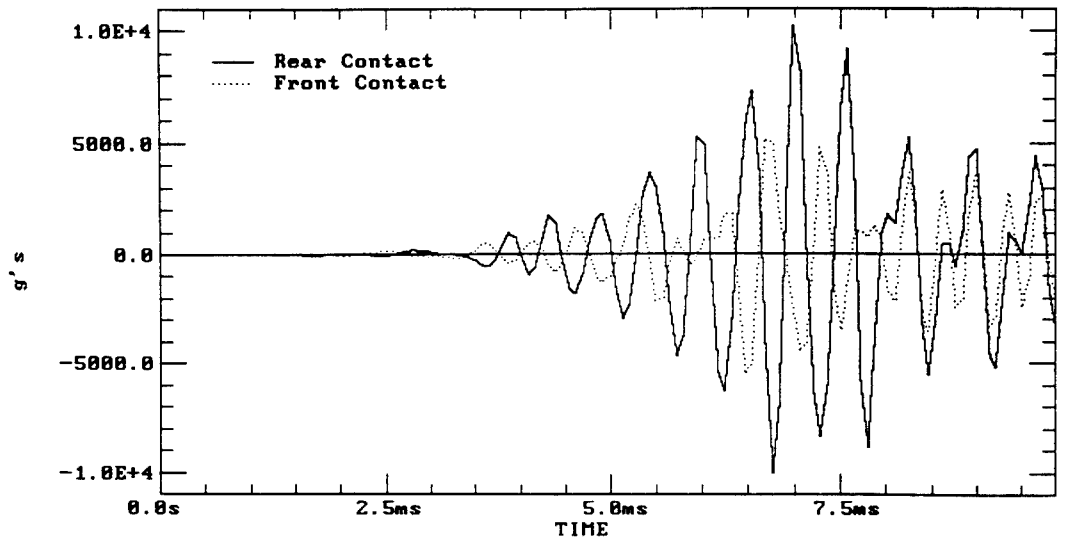

Figure B-3. Case 3 transverse acceleration from Task B gun - rail centerline.

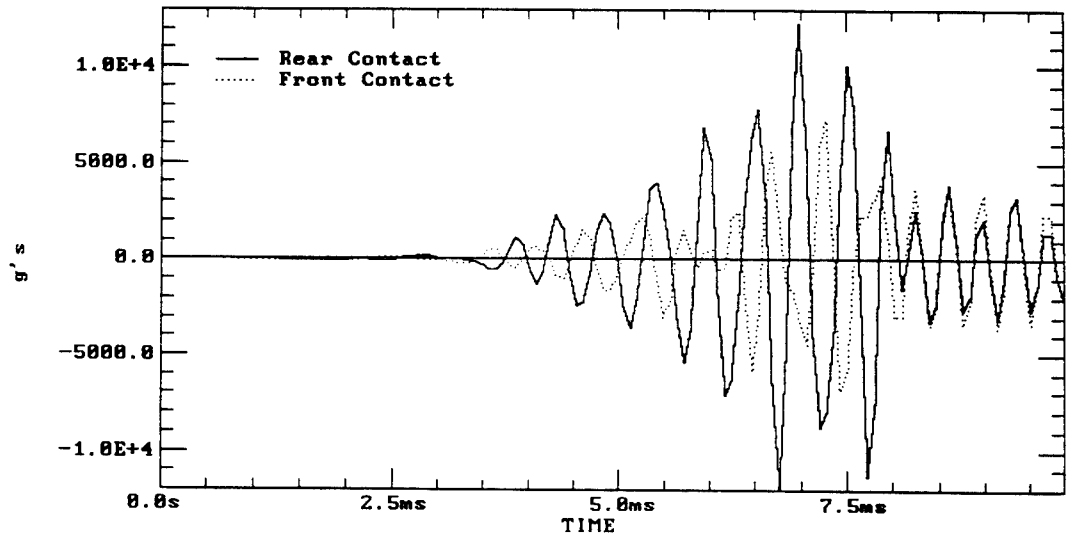

Figure B-4. Case 4 transverse acceleration from Task B gun - rail centerline.

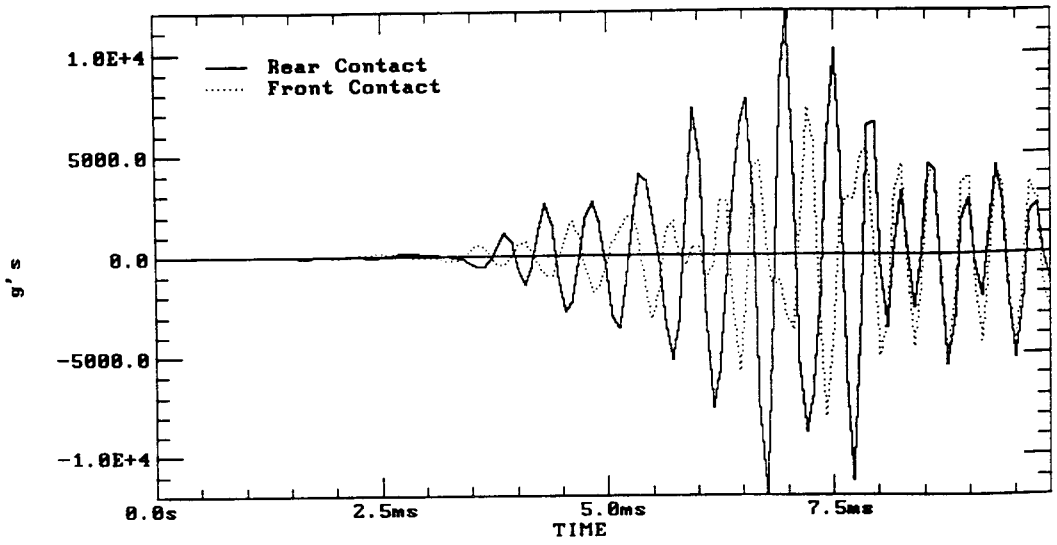

Figure B-5. Case 5 transverse acceleration from Task B gun - rail centerline.

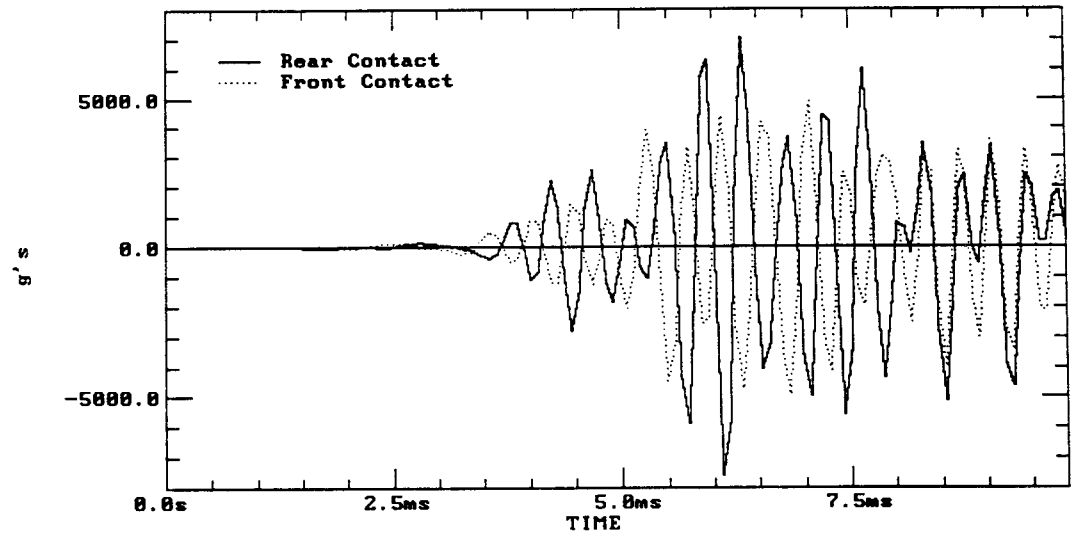

Figure B-6. Case 6 transverse acceleration from Task B gun - rail centerline.

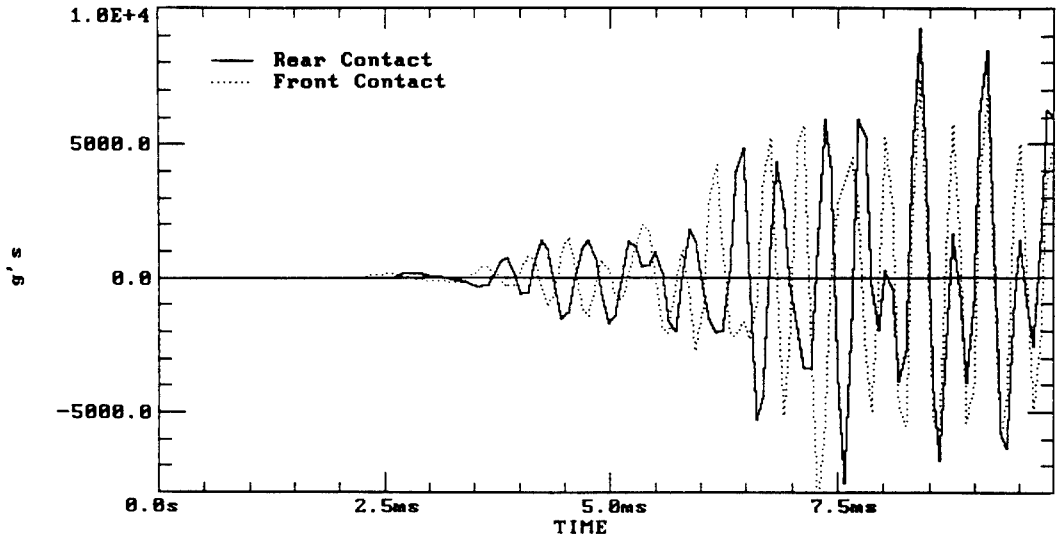

Figure B-7. Case 7 transverse acceleration from Task B gun - rail centerline.

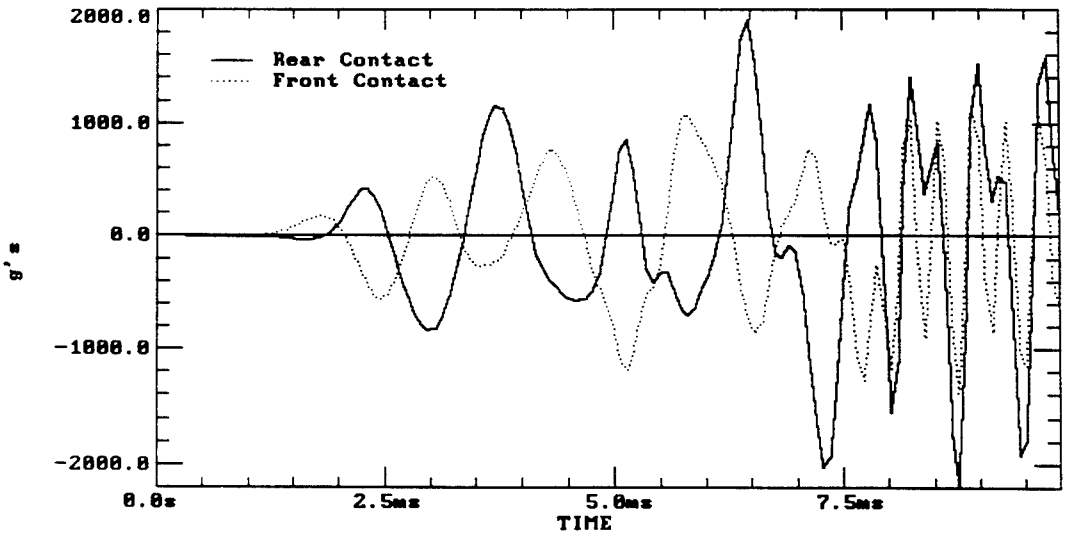

Figure B-8. Case 1 transverse acceleration from Task B gun insulator centerline.

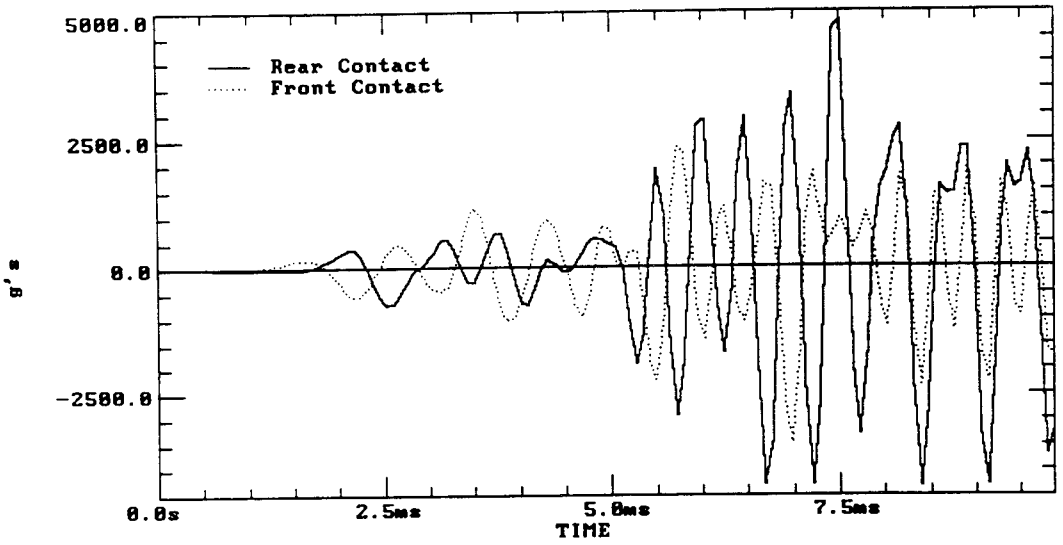

Figure B-9. Case 2 transverse acceleration from Task B gun insulator centerline.

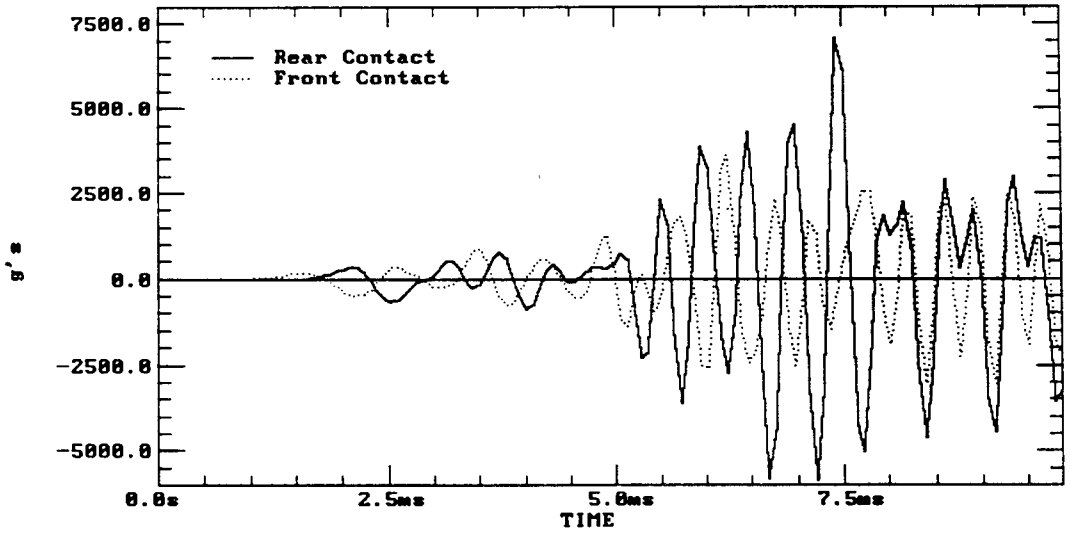

Figure B-10. Case 3 transverse acceleration from Task B gun insulator centerline.

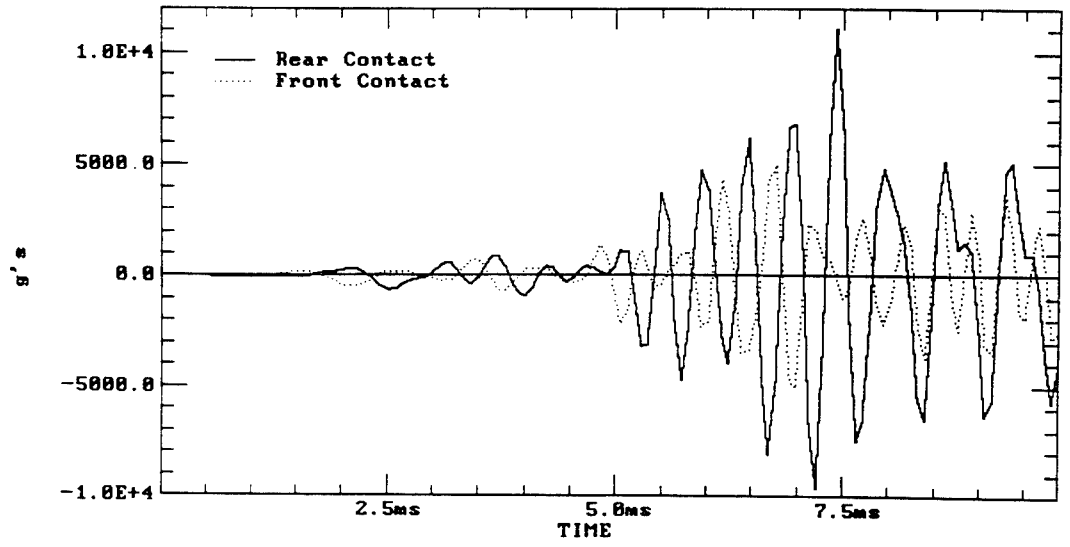

Figure B-11. Case 4 transverse acceleration from Task B gun insulator centerline.

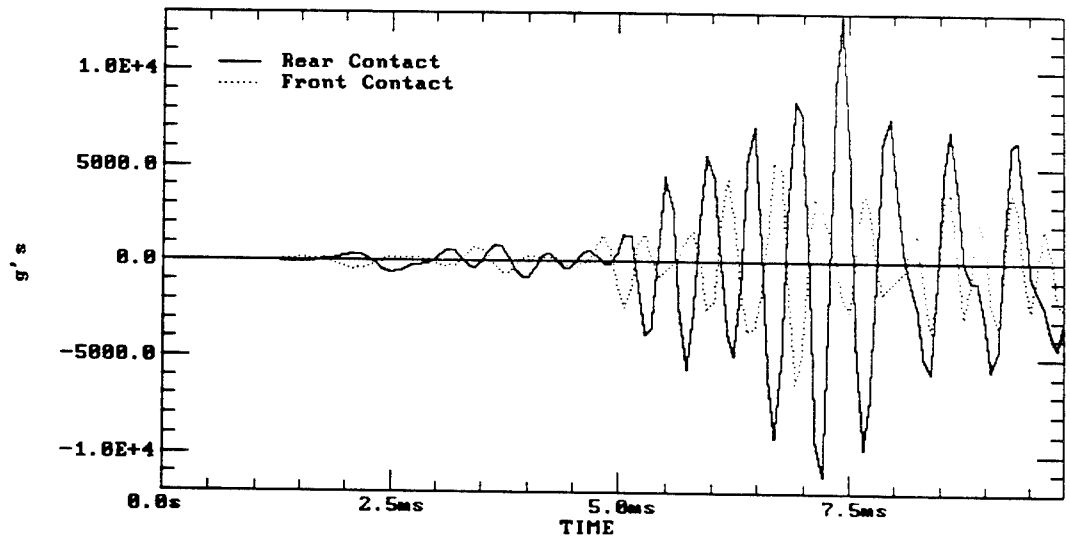

Figure B-12. Case 5 transverse acceleration from Task B gun insulator centerline.

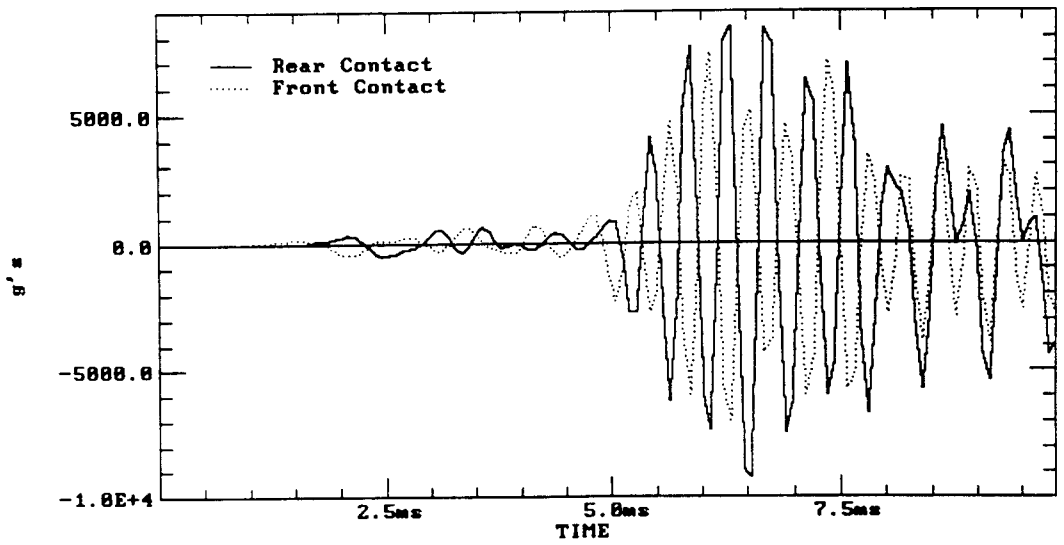

Figure B-13. Case 6 transverse acceleration from Task B gun insulator centerline.

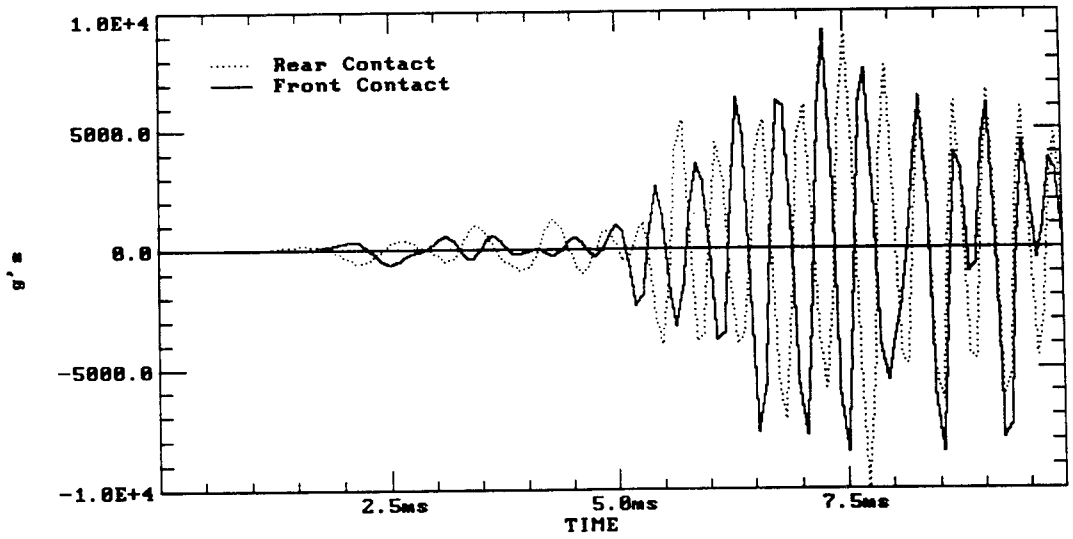

Figure B-14. Case 7 transverse acceleration from Task B gun insulator centerline.

INTENTIONALLY LEFT BLANK.

APPENDIX C:

ANGULAR ACCELERATION PLOTS FOR TASK B GUN

INTENTIONALLY LEFT BLANK.

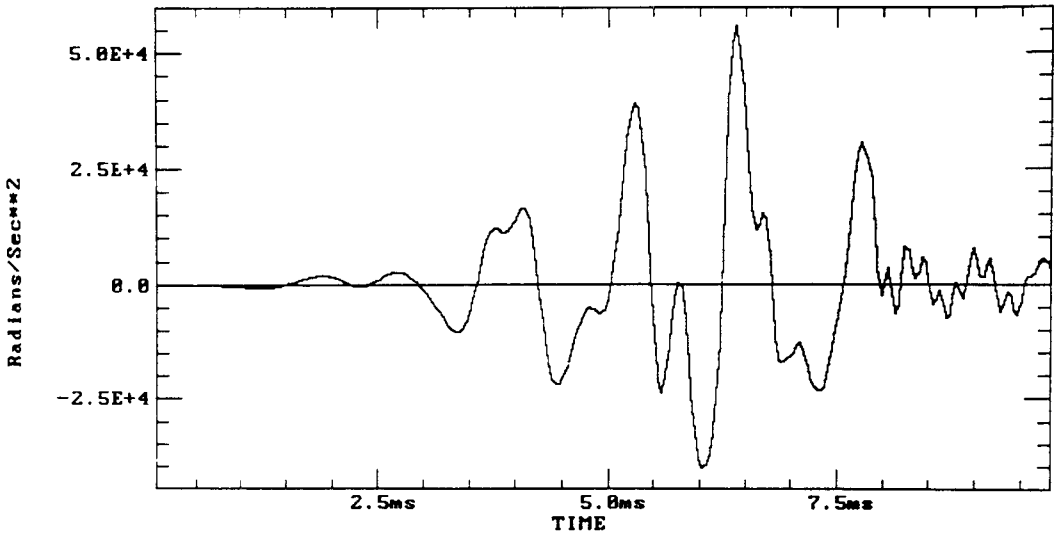

Figure C-1. Case 1 angular acceleration from Task B gun - rail centerline.

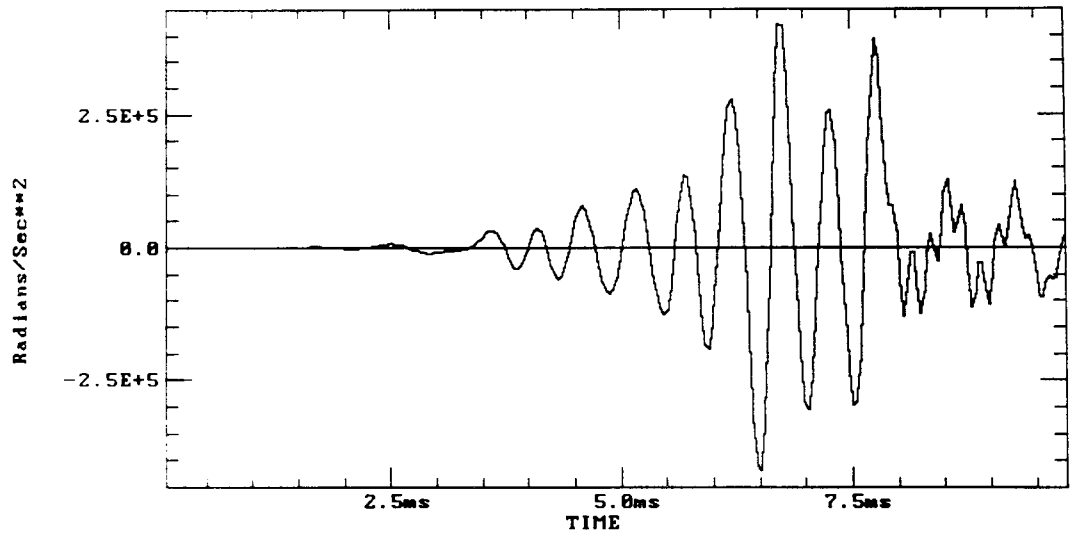

Figure C-2. Case 2 angular acceleration from Task B gun - rail centerline.

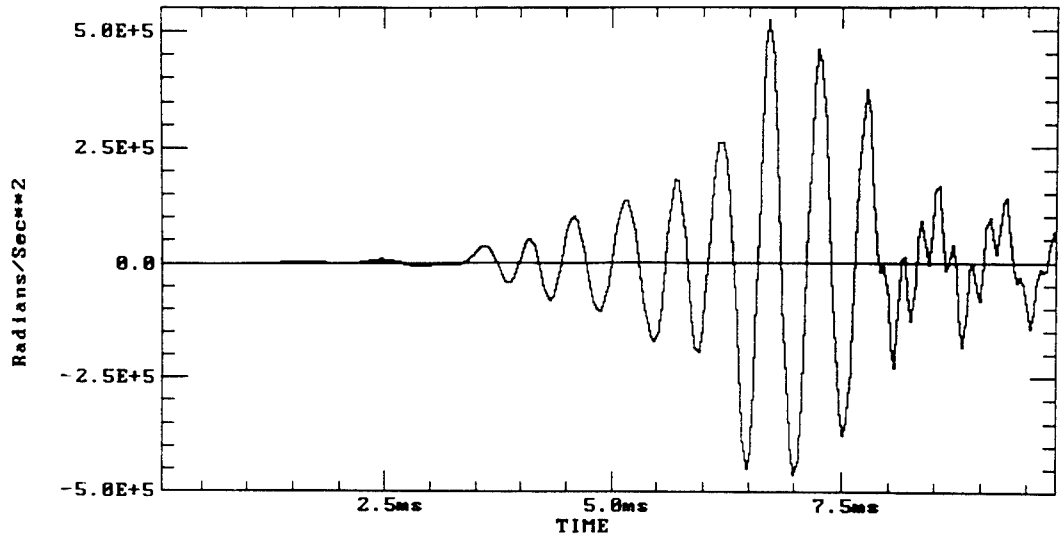

Figure C-3. Case 3 angular acceleration from Task B gun - rail centerline.

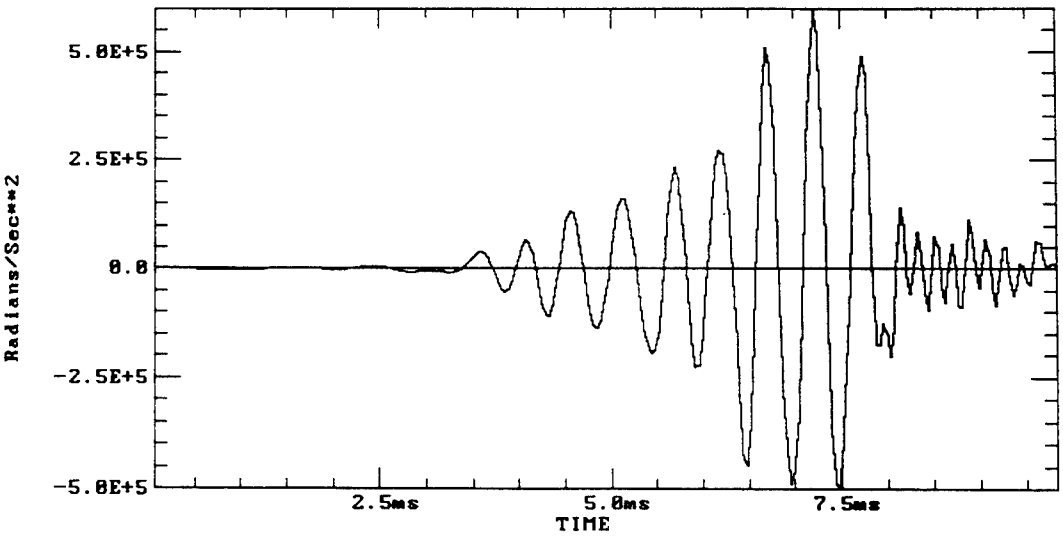

Figure C-4. Case 4 angular acceleration from Task B gun - rail centerline.

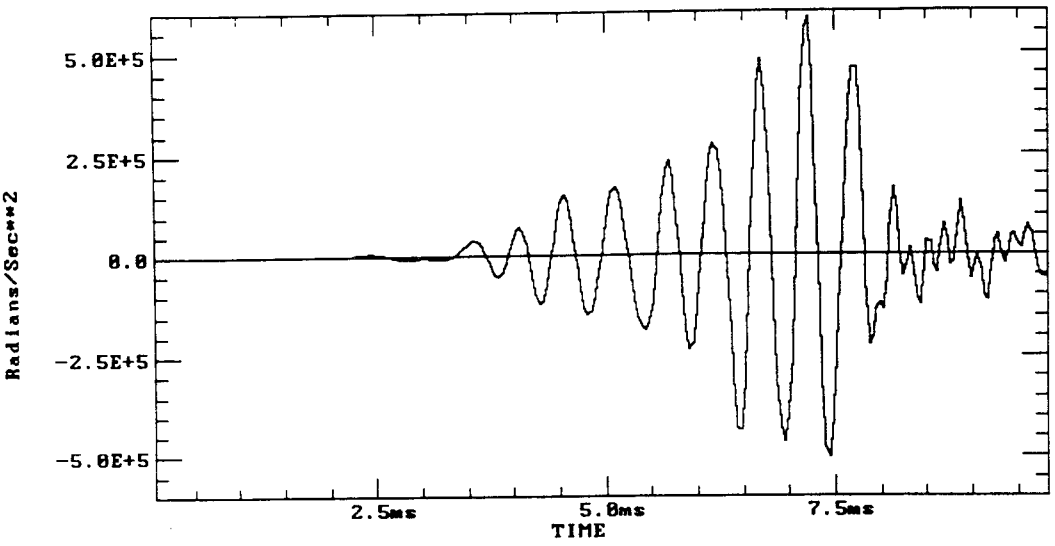

Figure C-5. Case 5 angular acceleration from Task B gun - rail centerline.

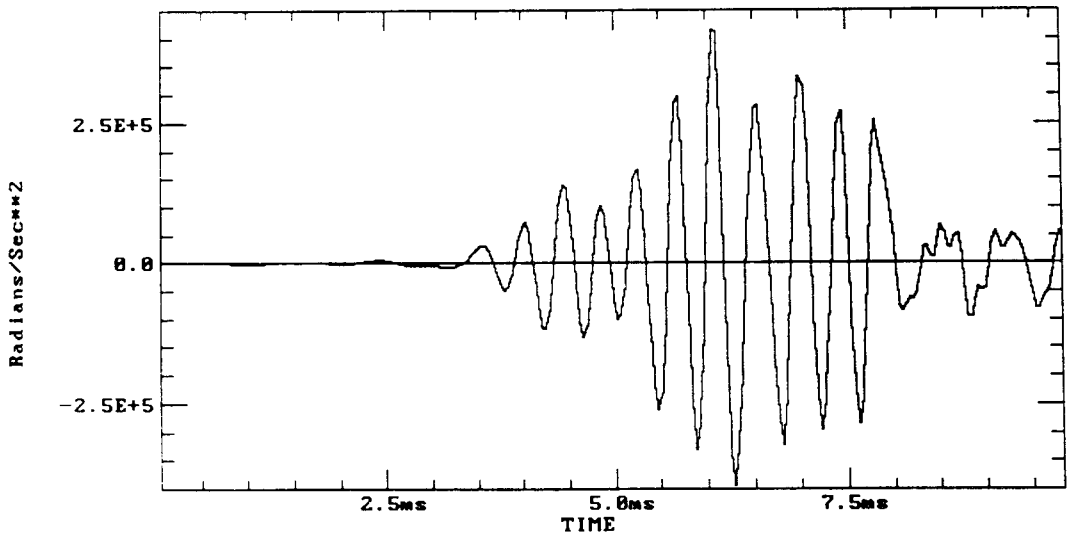

Figure C-6. Case 6 angular acceleration from Task B gun - rail centerline.

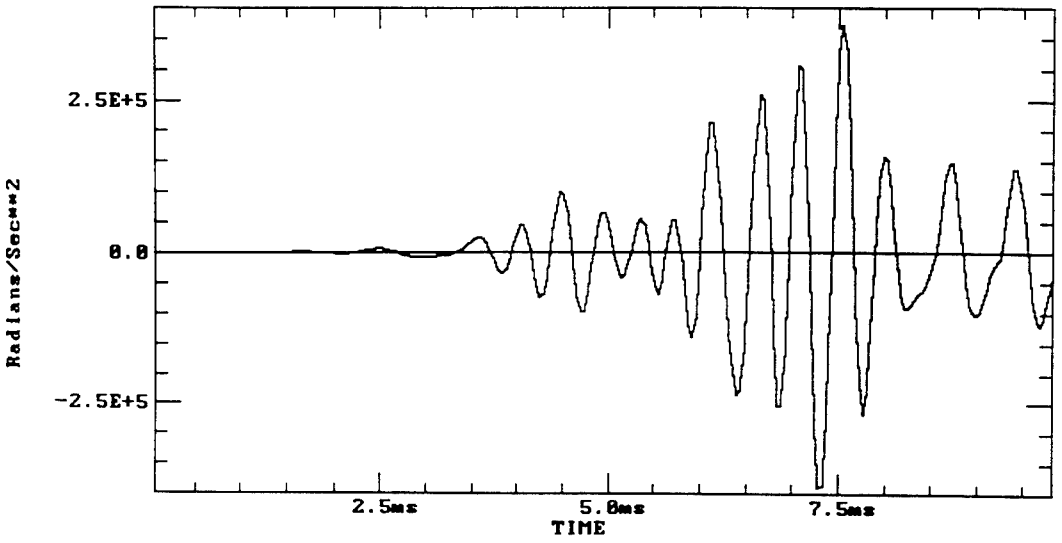

Figure C-7. Case 7 angular acceleration from Task B gun - rail centerline.

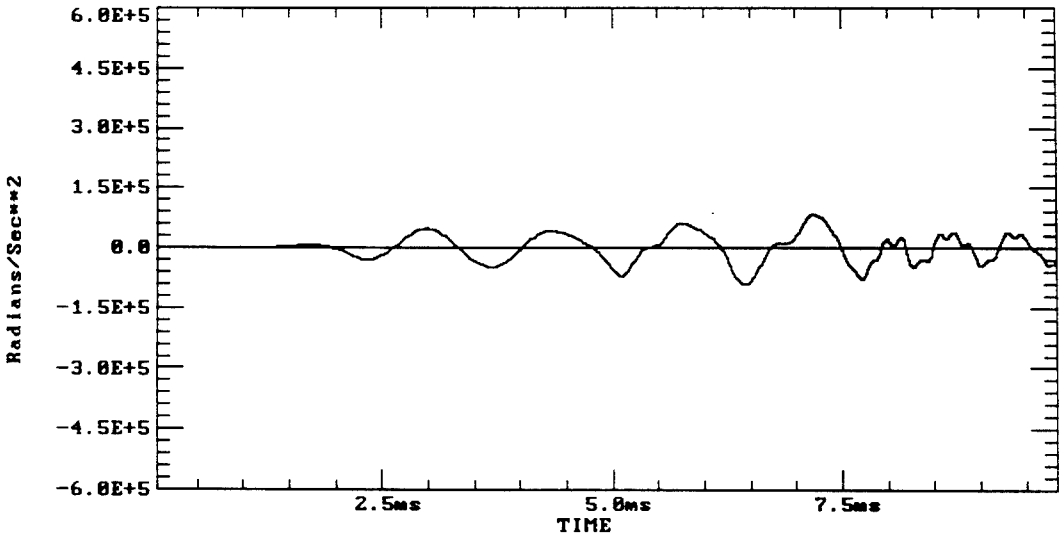

Figure C-8. Case 1 angular acceleration from Task B gun insulator centerline.

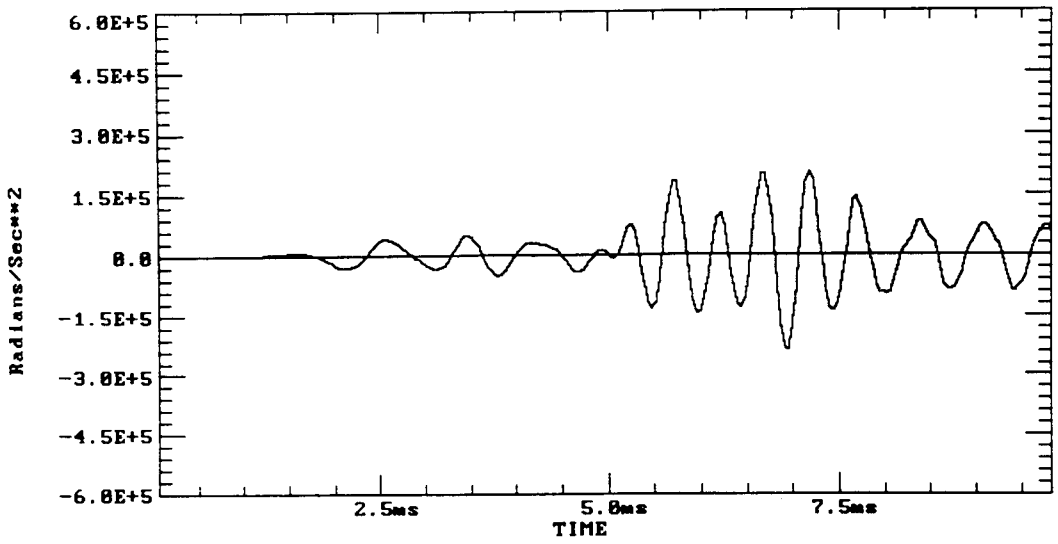

Figure C-9. Case 2 angular acceleration from Task B gun insulator centerline.

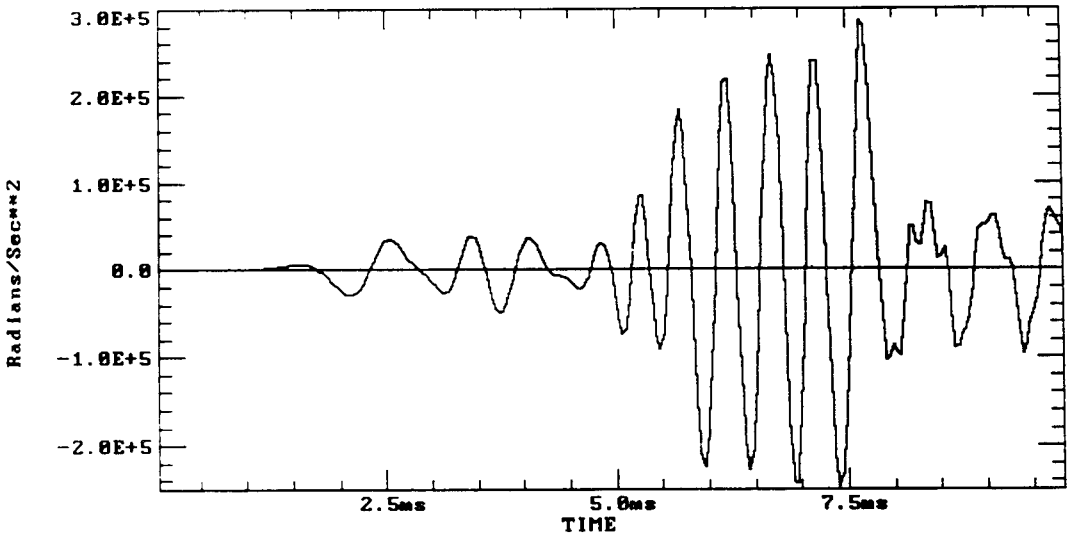

Figure C-10. Case 3 angular acceleration from Task B gun insulator centerline.

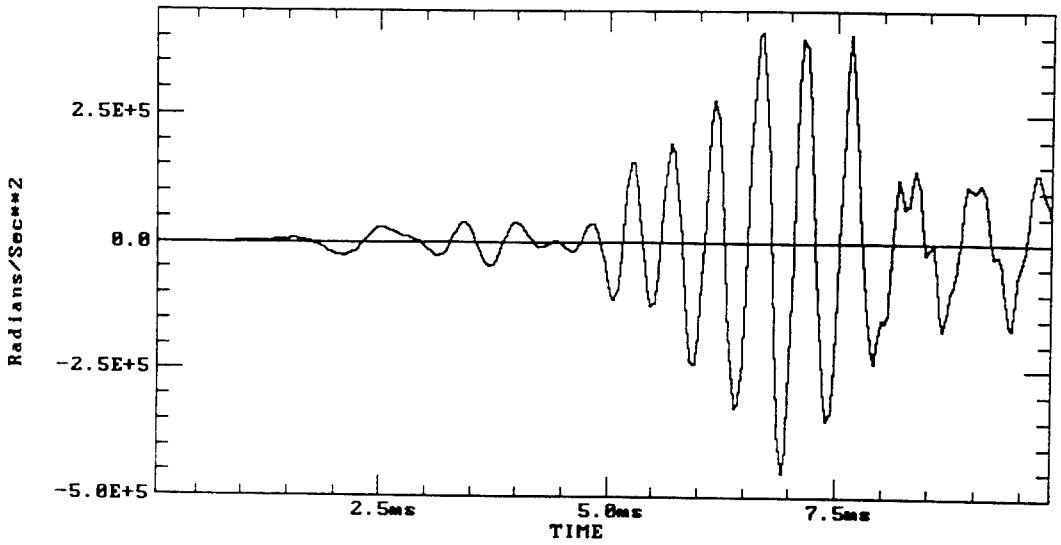

Figure C-11. Case 4 angular acceleration from Task B gun insulator centerline.

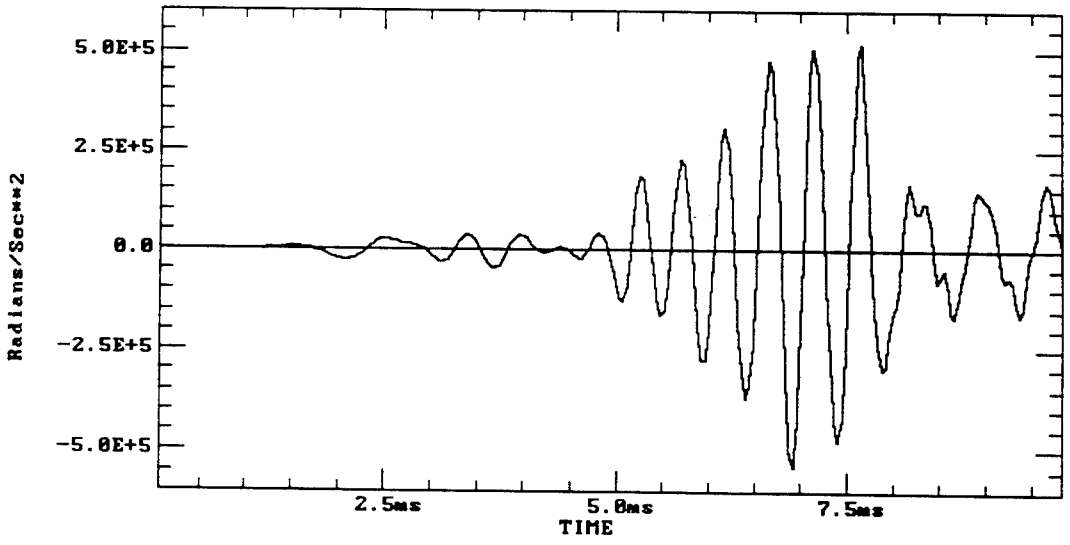

Figure C-12. Case 5 angular acceleration from Task B gun insulator centerline.

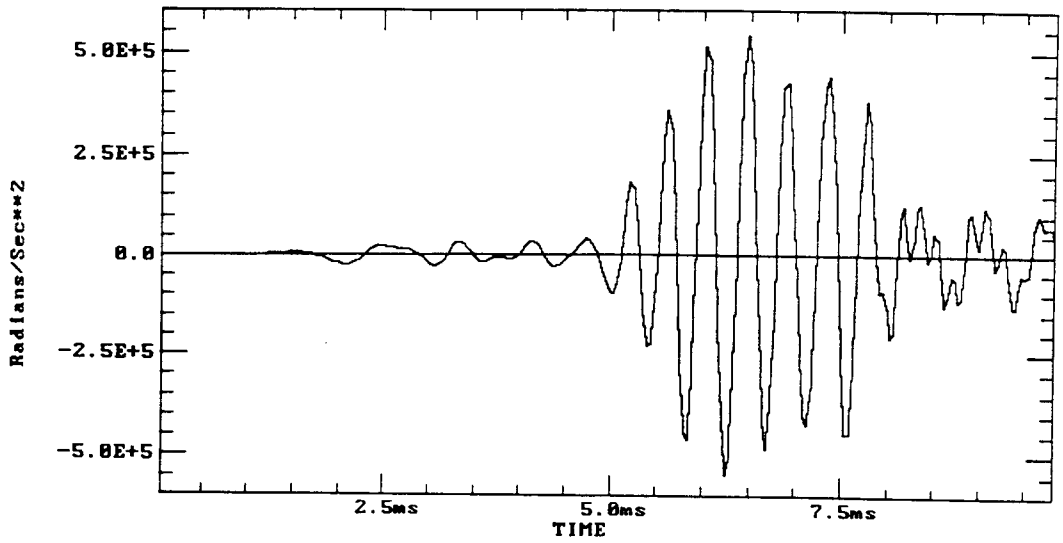

Figure C-13. Case 6 angular acceleration from Task B gun insulator centerline.

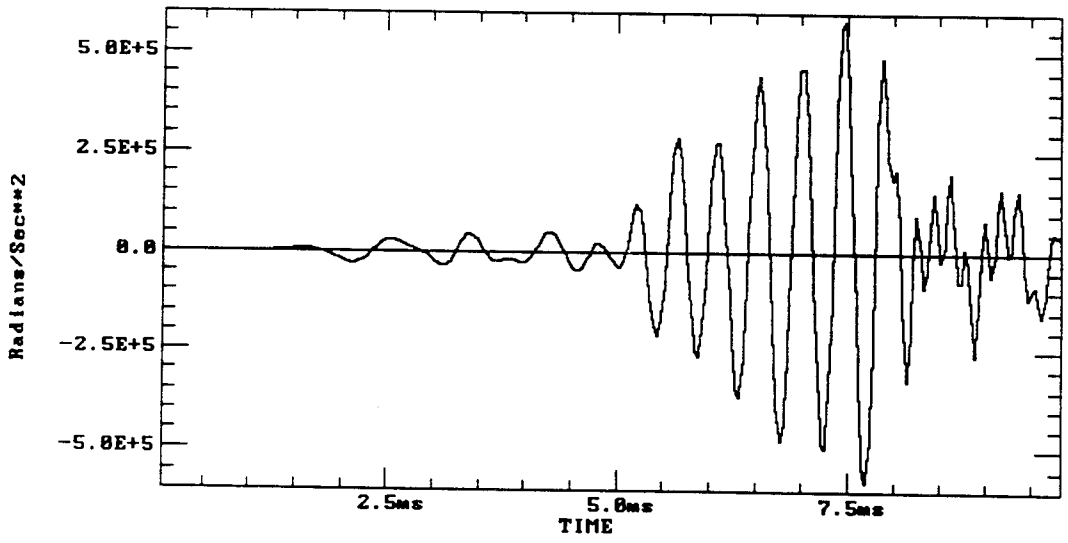

Figure C-14. Case 7 angular acceleration from Task B gun insulator centerline.

INTENTIONALLY LEFT BLANK.

APPENDIX D:

TRANSVERSE ACCELERATION PLOTS FOR TASK C GUN

INTENTIONALLY LEFT BLANK.

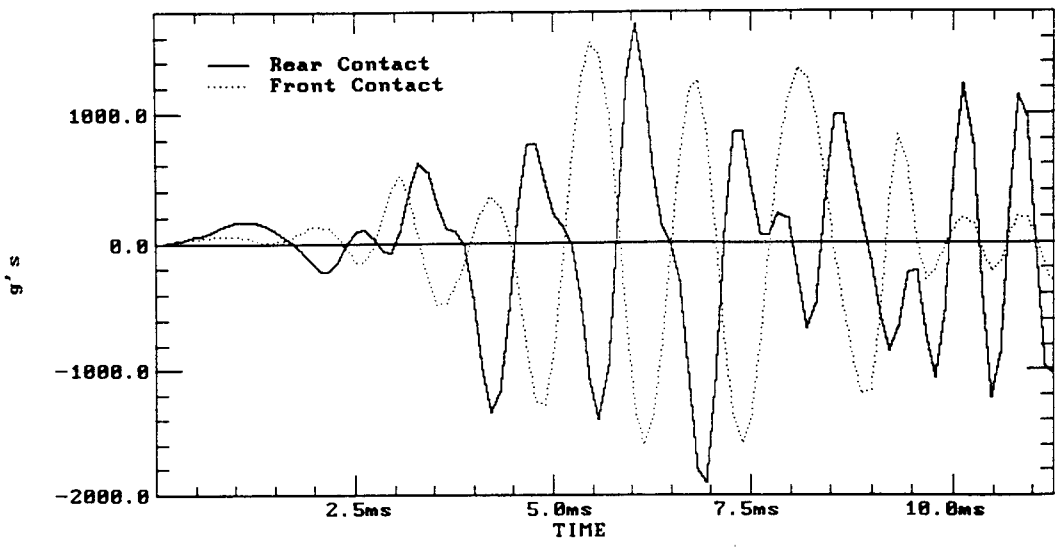

Figure D-1. Case 1 transverse acceleration from Task C gun - rail centerline.

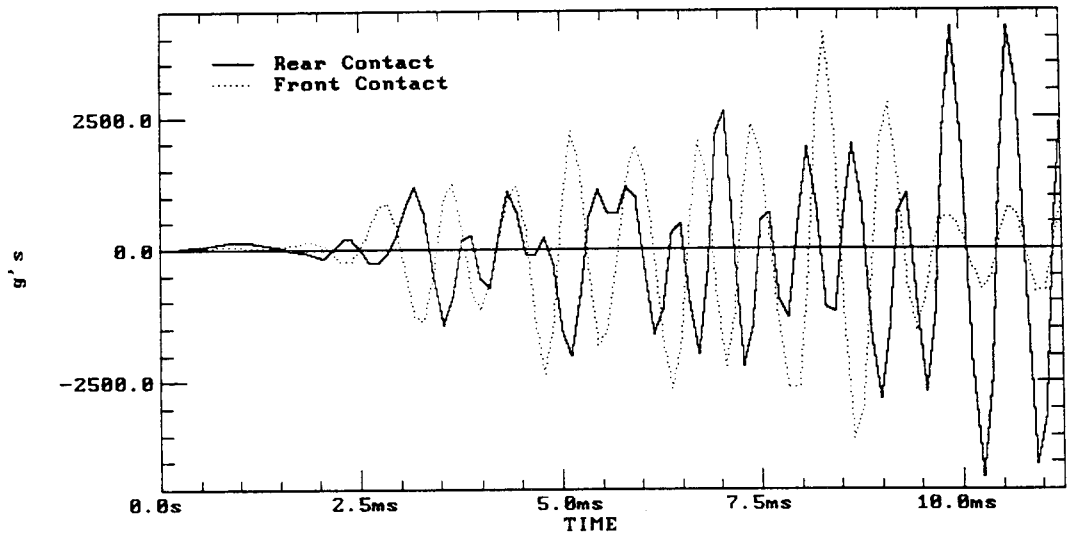

Figure D-2. Case 2 transverse acceleration from Task C gun - rail centerline.

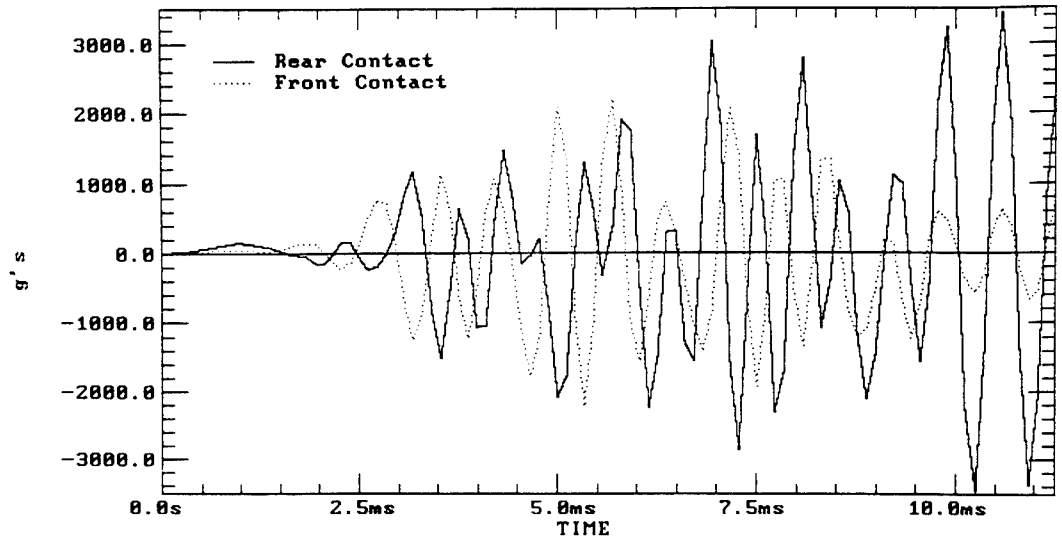

Figure D-3. Case 3 transverse acceleration from Task C gun - rail centerline.

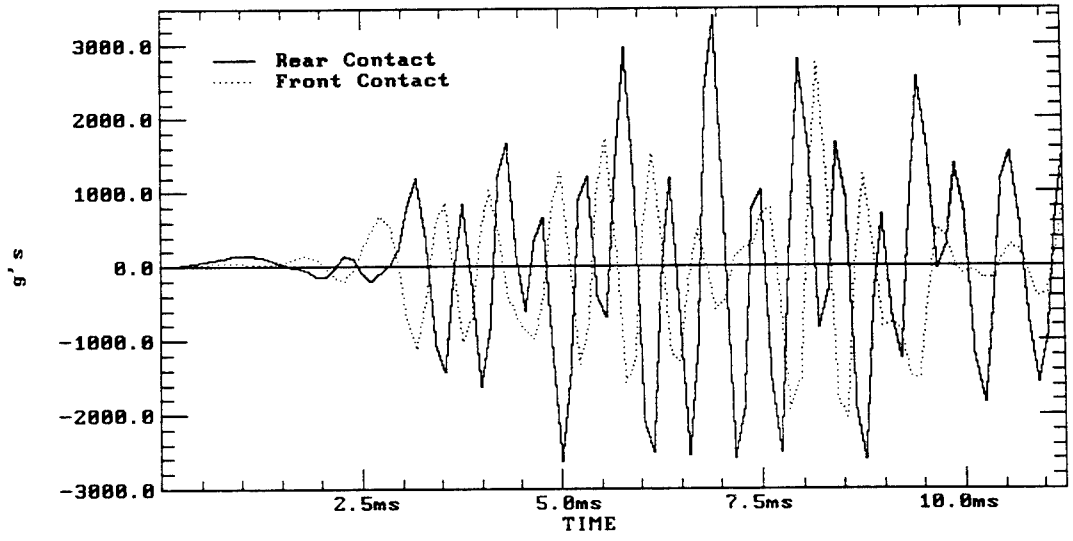

Figure D-4. Case 4 transverse acceleration from Task C gun - rail centerline.

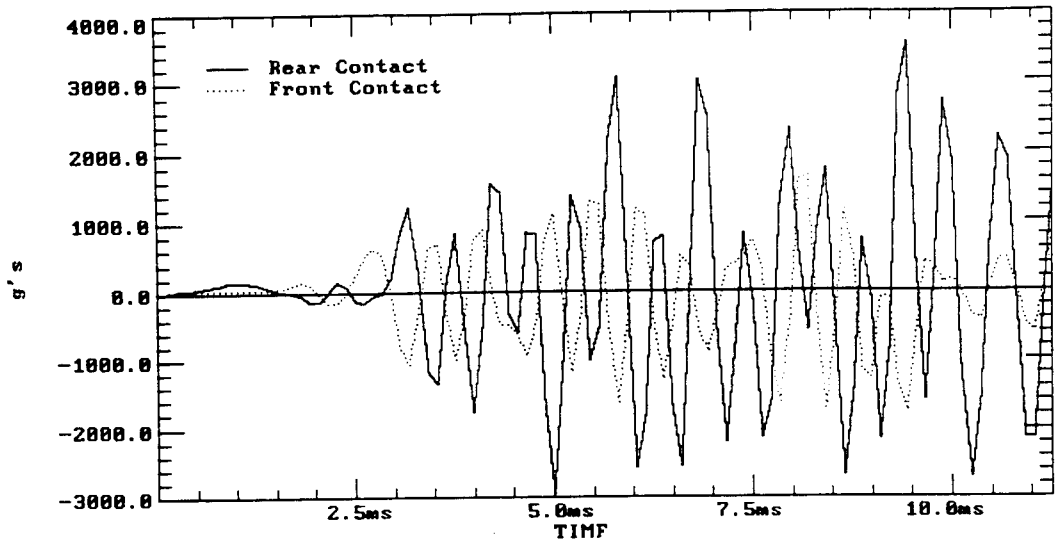

Figure D-5. Case 5 transverse acceleration from Task C gun - rail centerline.

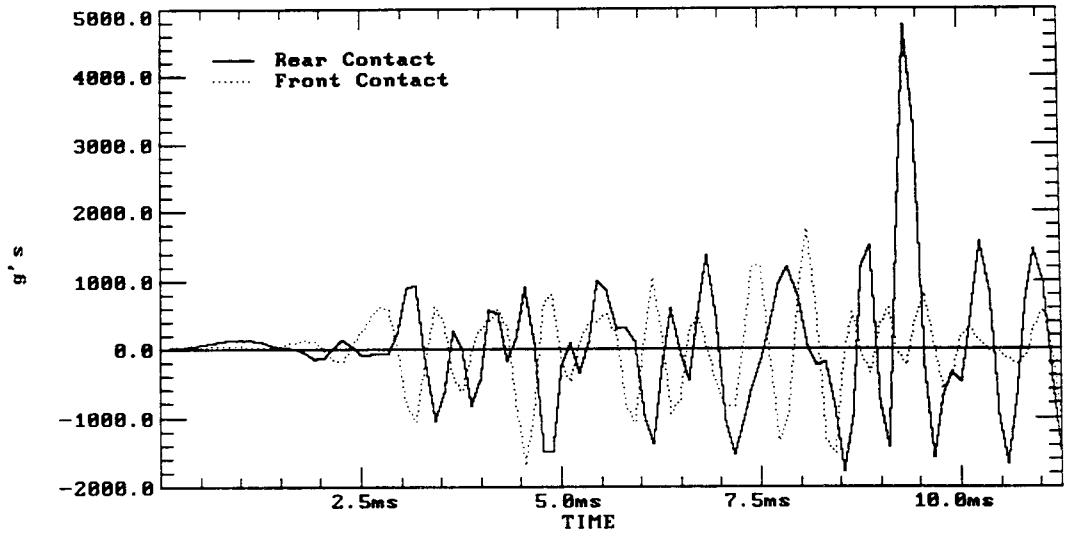

Figure D-6. Case 6 transverse acceleration from Task C gun - rail centerline.

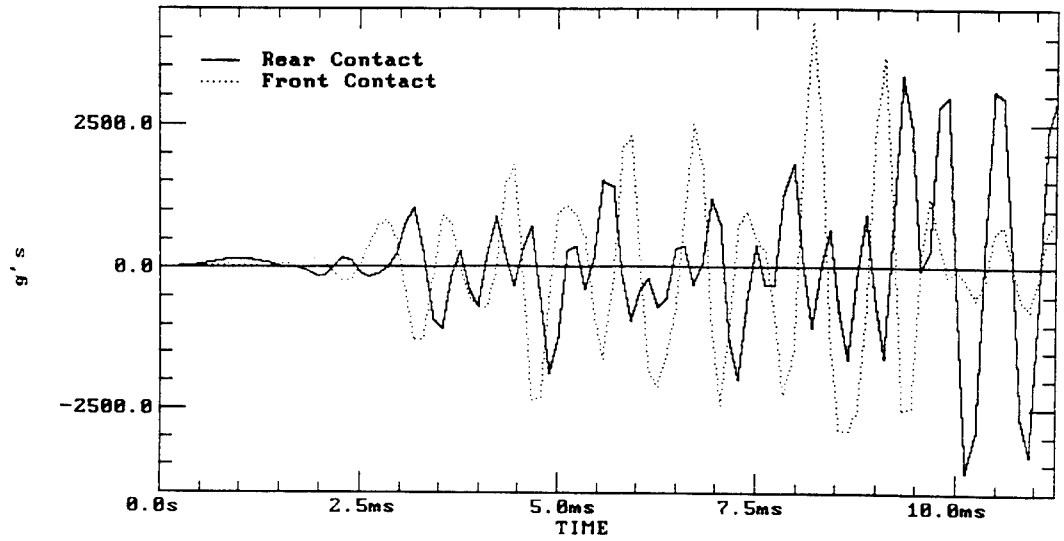

Figure D-7. Case 7 transverse acceleration from Task C gun - rail centerline.

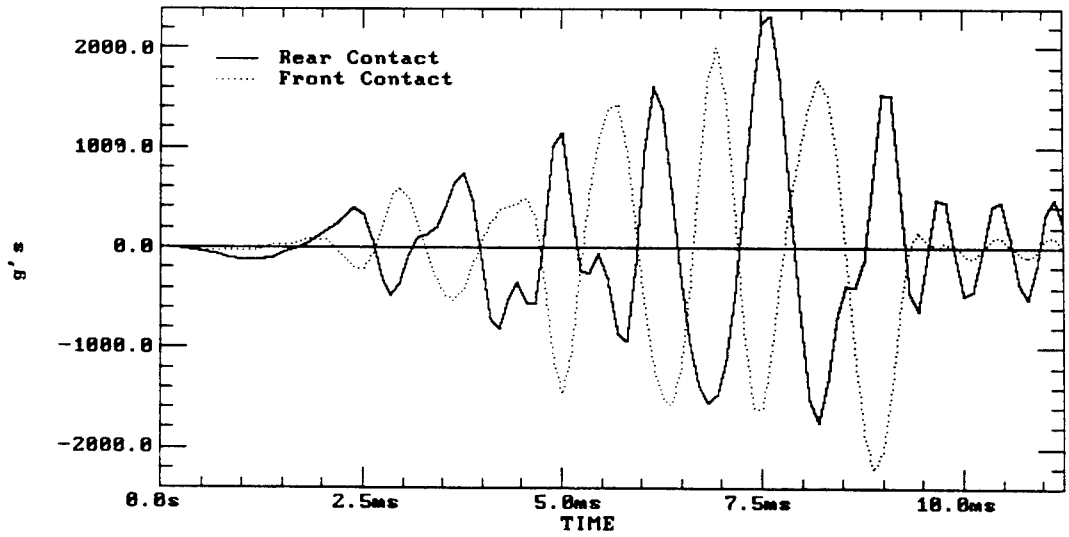

Figure D-8. Case 1 transverse acceleration from Task C gun insulator centerline.

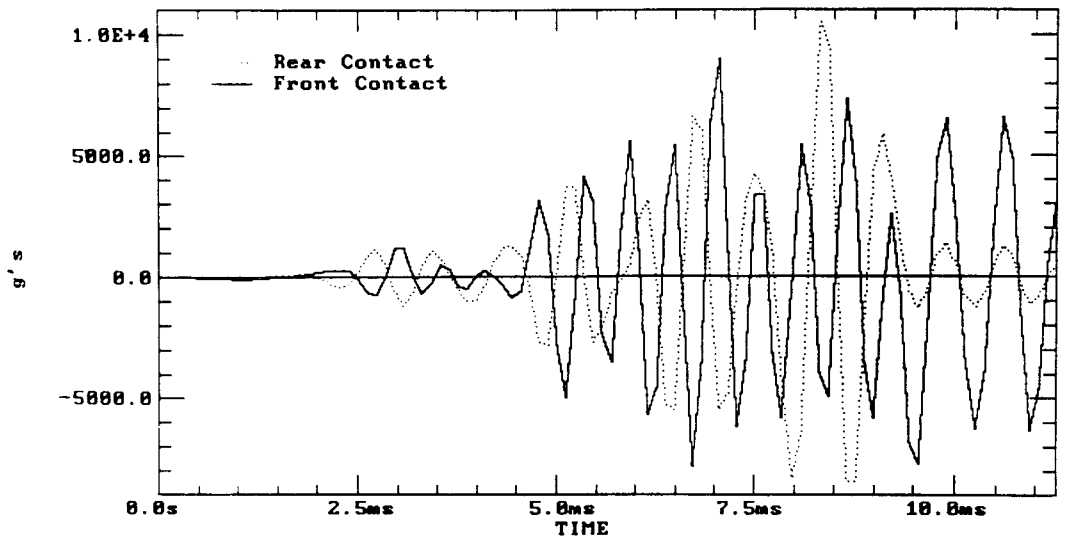

Figure D-9. Case 2 transverse acceleration from Task C gun insulator centerline.

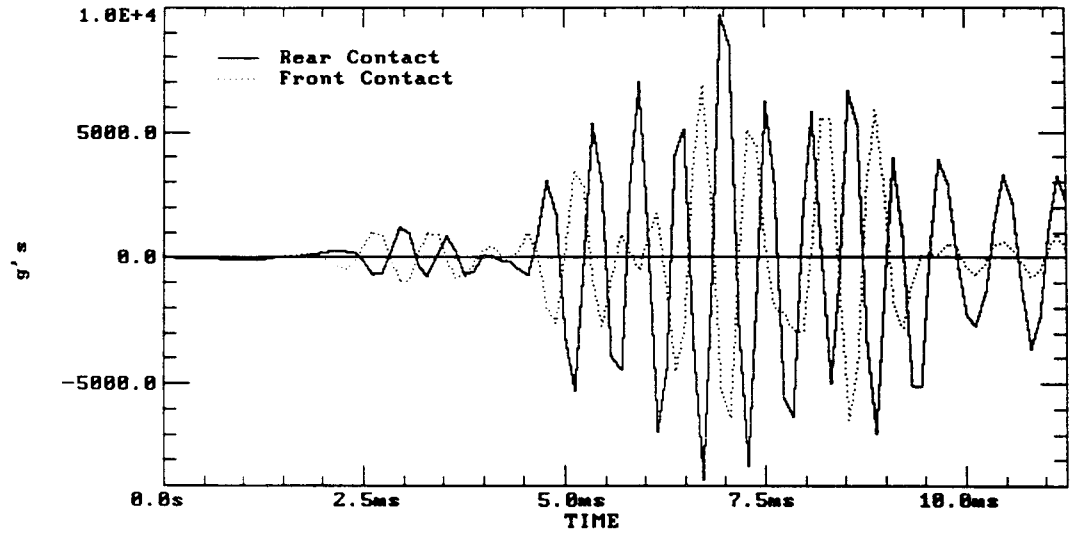

Figure D-10. Case 3 transverse acceleration from Task C gun insulator centerline.

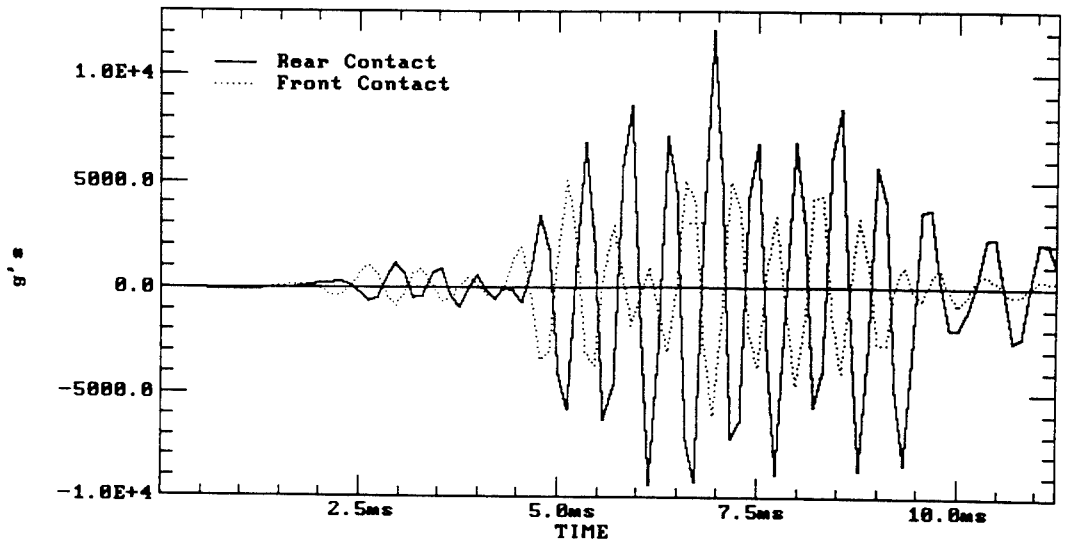

Figure D-11. Case 4 transverse acceleration from Task C gun insulator centerline.

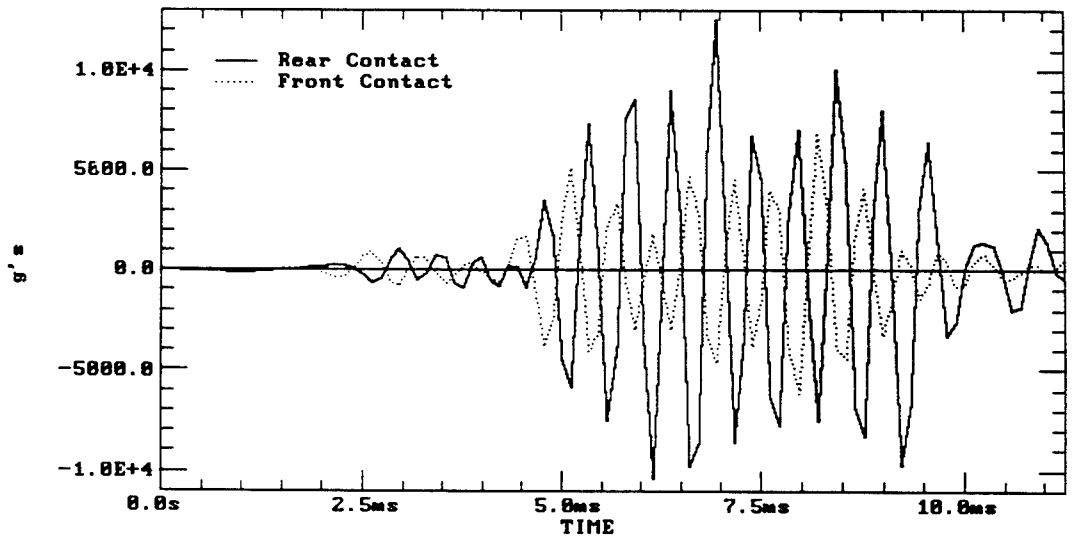

Figure D-12. Case 5 transverse acceleration from Task C gun insulator centerline.

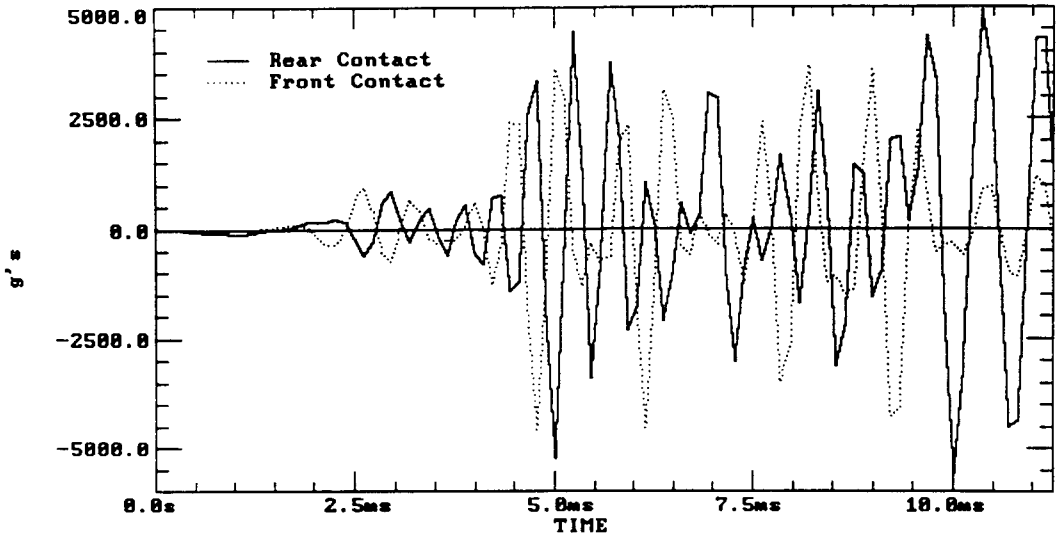

Figure D-13. Case 6 transverse acceleration from Task C gun insulator centerline.

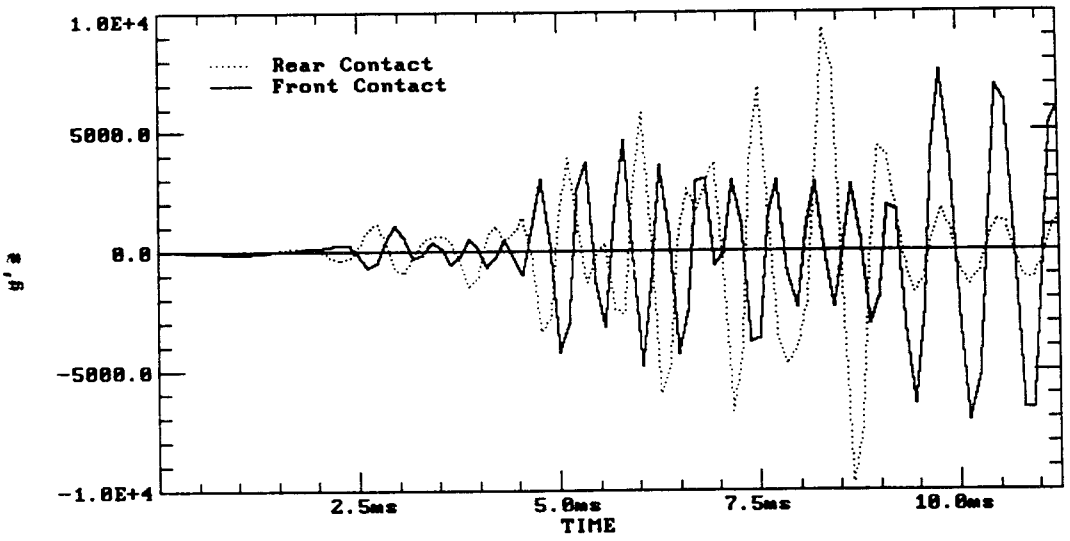

Figure D-14. Case 7 transverse acceleration from Task C gun insulator centerline.

INTENTIONALLY LEFT BLANK.

APPENDIX E:

ANGULAR ACCELERATION PLOTS FOR TASK C GUN

INTENTIONALLY LEFT BLANK.

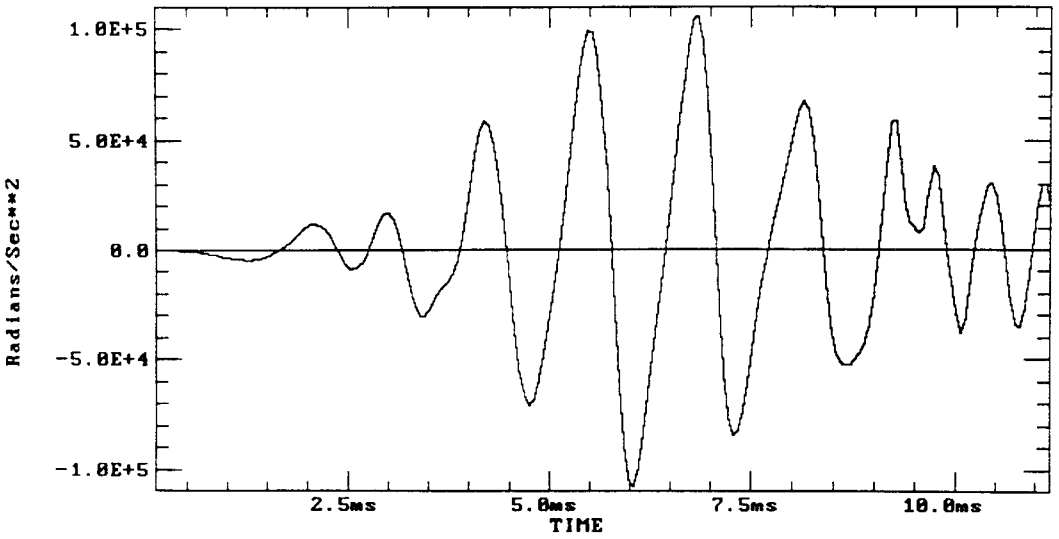

Figure E-1. Case 1 angular acceleration from Task C gun - rail centerline.

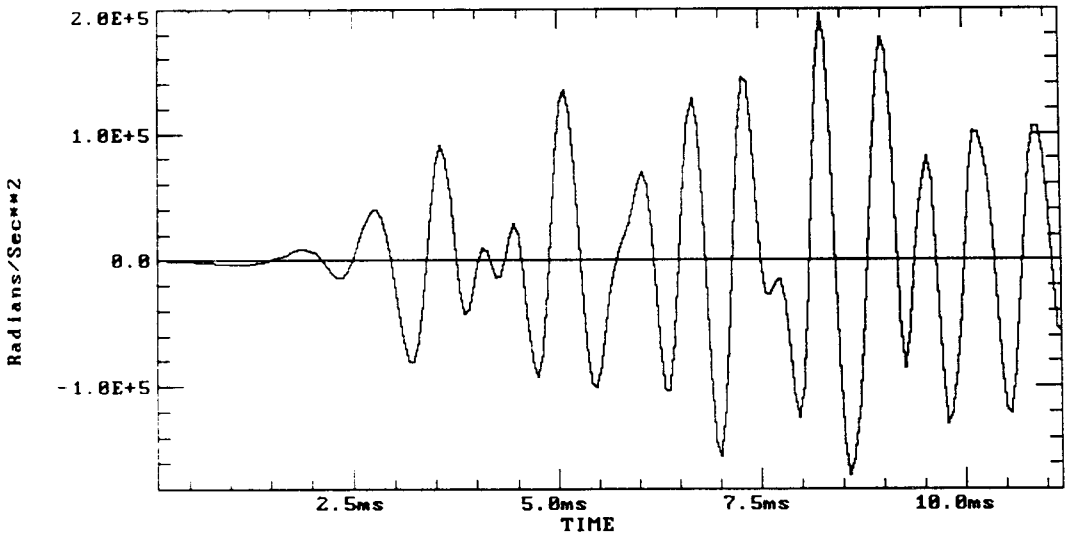

Figure E-2. Case 2 angular acceleration from Task C gun - rail centerline.

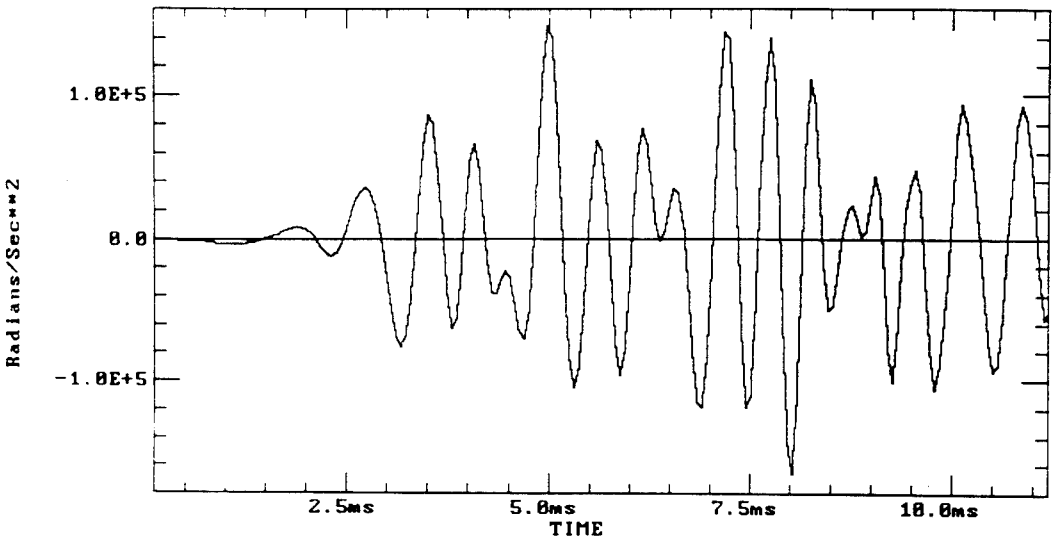

Figure E-3. Case 3 angular acceleration from Task C gun - rail centerline.

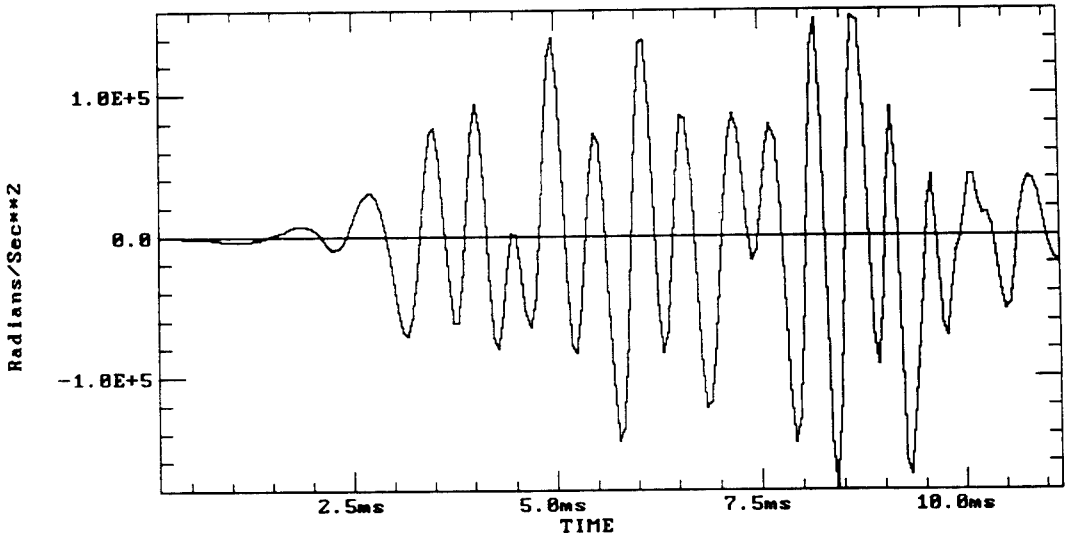

Figure E-4. Case 4 angular acceleration from Task C gun - rail centerline.

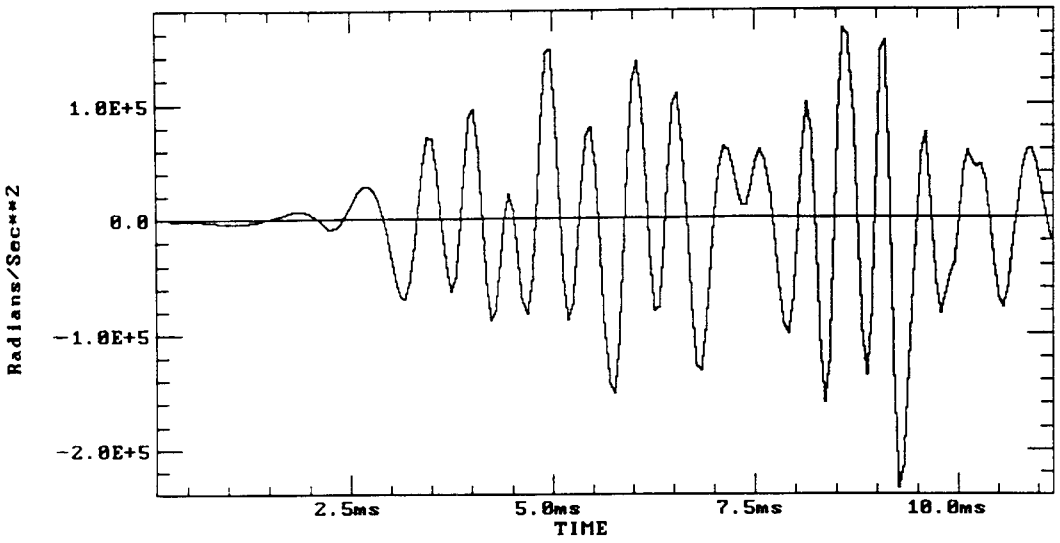

Figure E-5. Case 5 angular acceleration from Task C gun - rail centerline.

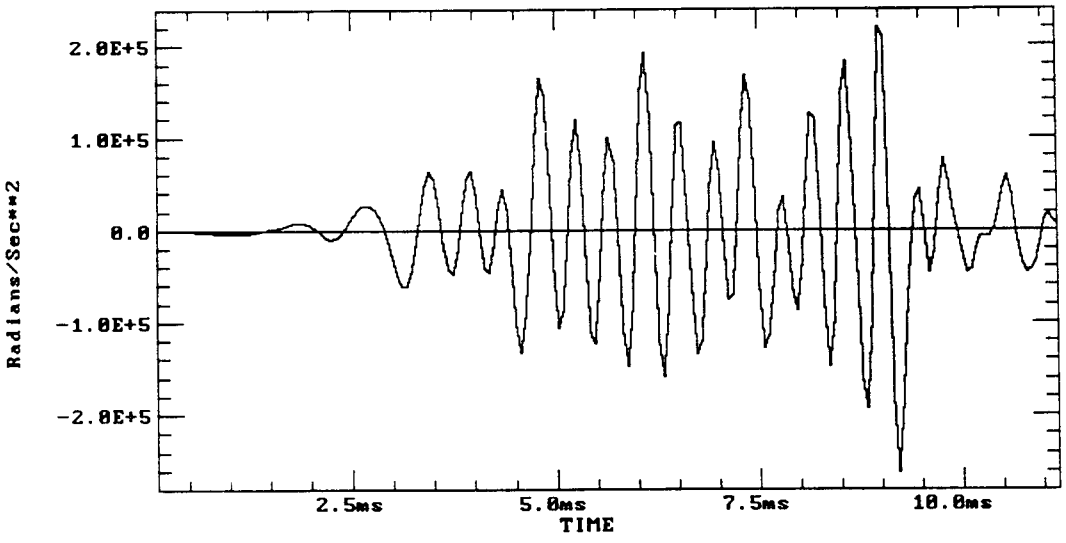

Figure E-6. Case 6 angular acceleration from Task C gun - rail centerline.

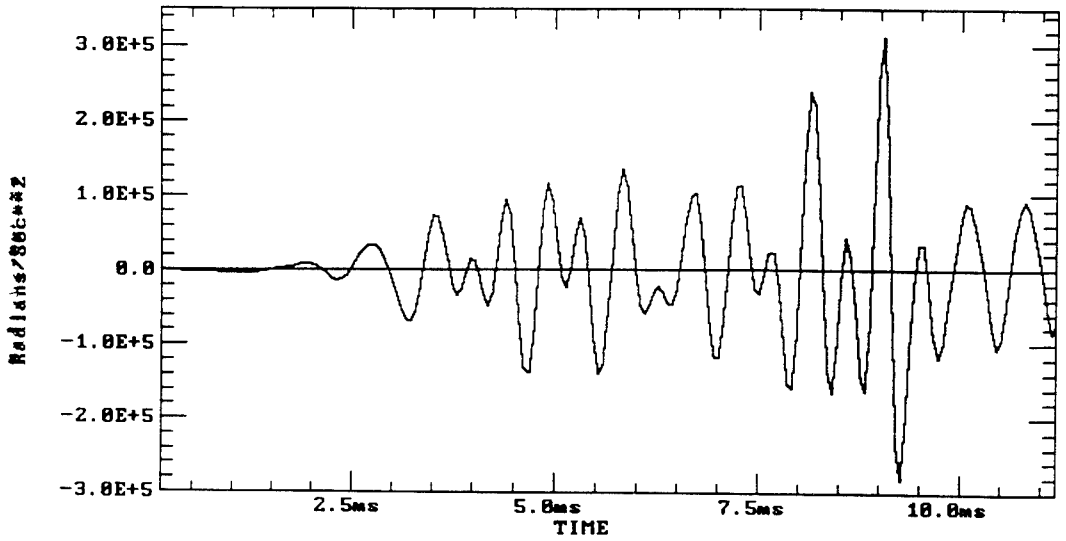

Figure E-7. Case 7 angular acceleration from Task C gun - rail centerline.

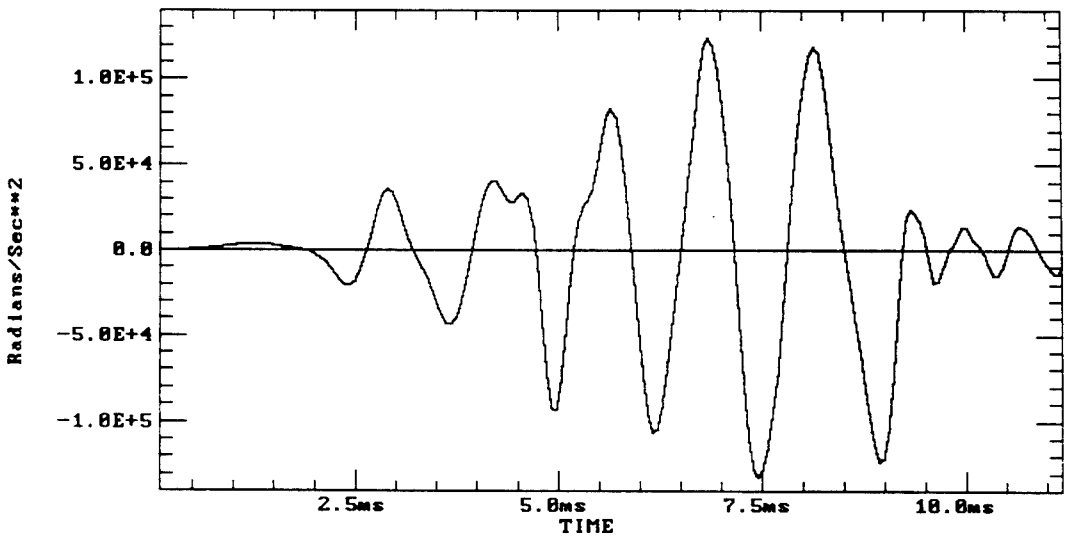

Figure E-8. Case 1 angular acceleration from Task C gun insulator centerline.

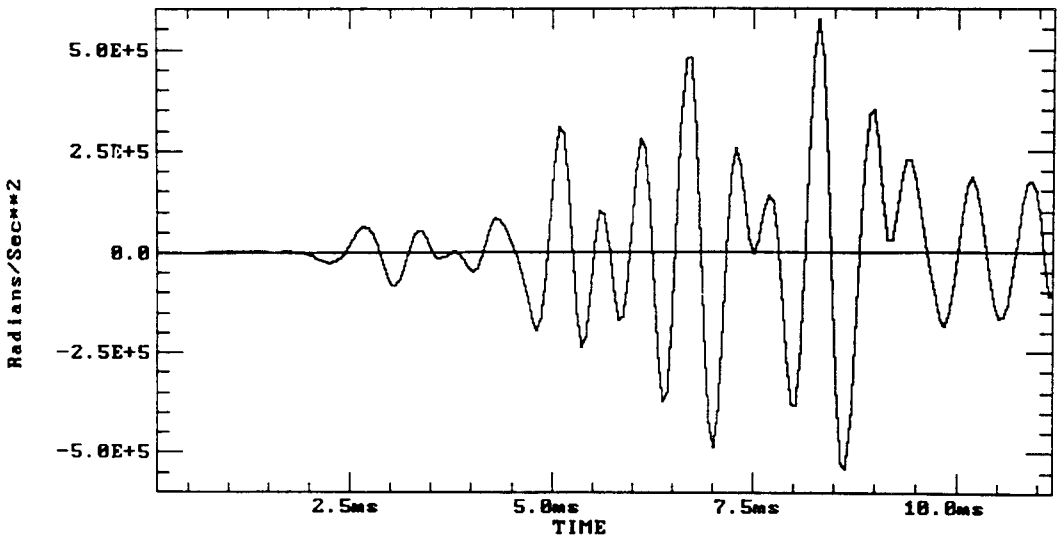

Figure E-9. Case 2 angular acceleration from Task C gun insulator centerline.

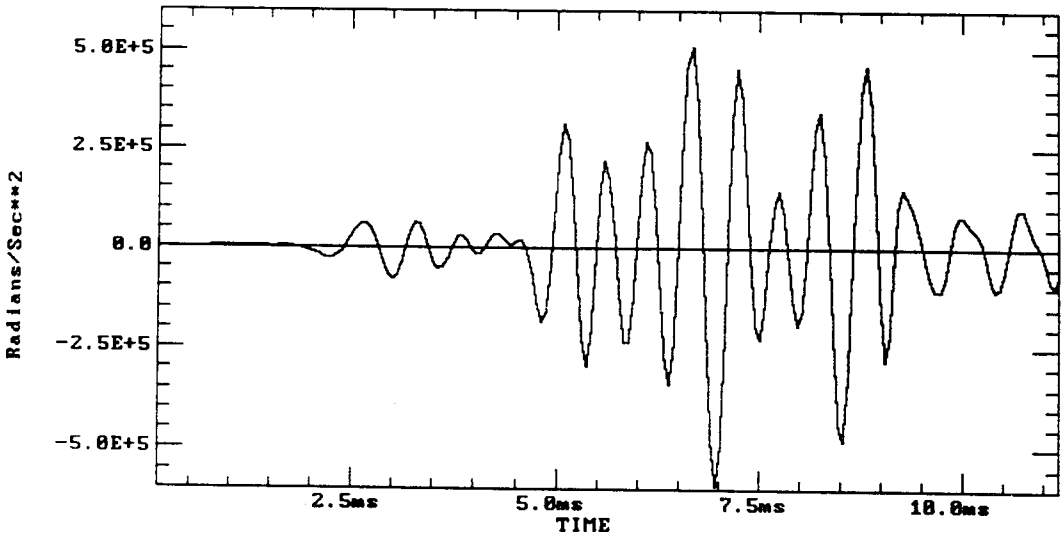

Figure E-10. Case 3 angular acceleration from Task C gun insulator centerline.

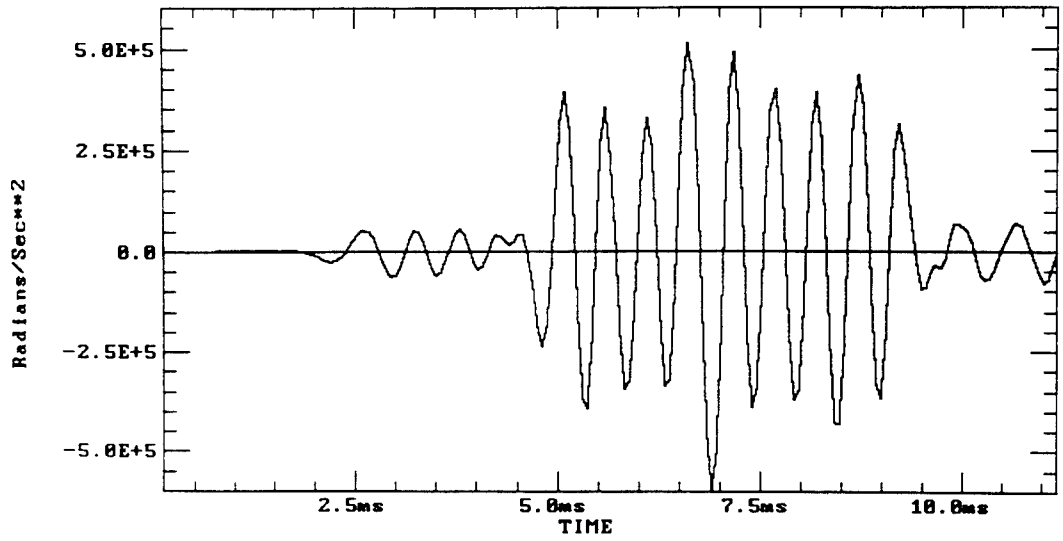

Figure E-11. Case 4 angular acceleration from Task C gun insulator centerline.

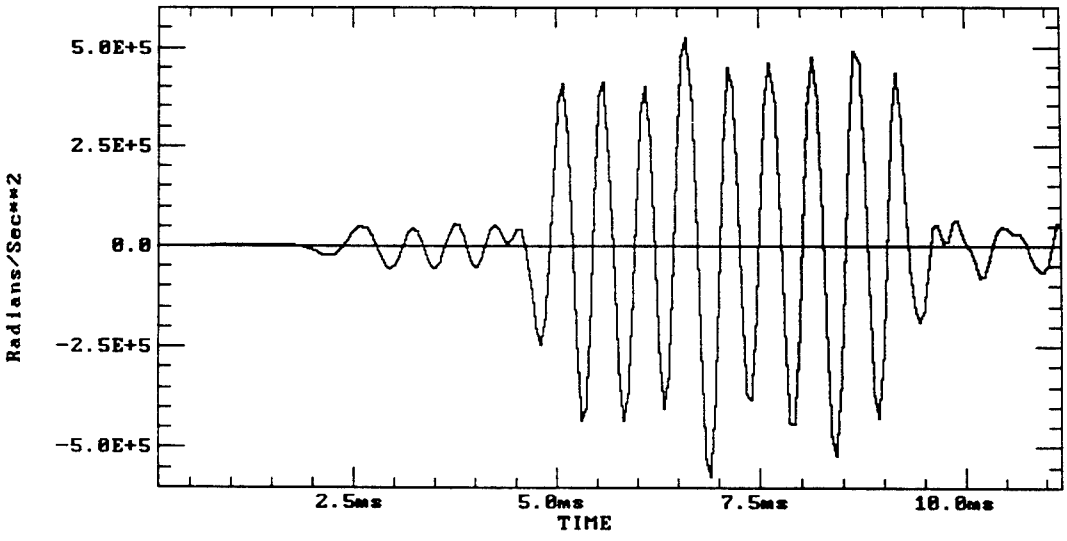

Figure E-12. Case 5 angular acceleration from Task C gun insulator centerline.

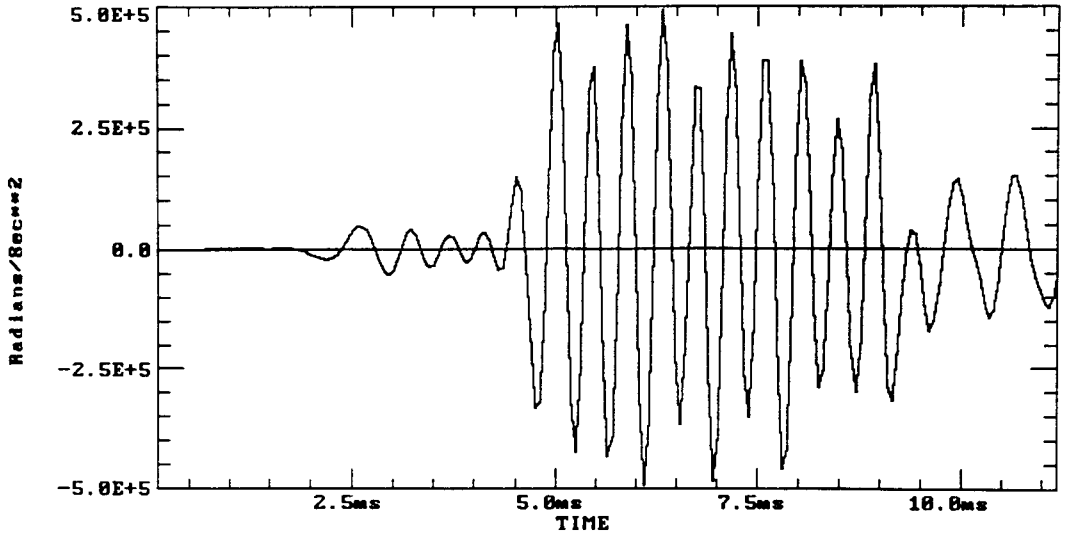

Figure E-13. Case 6 angular acceleration from Task C gun insulator centerline.

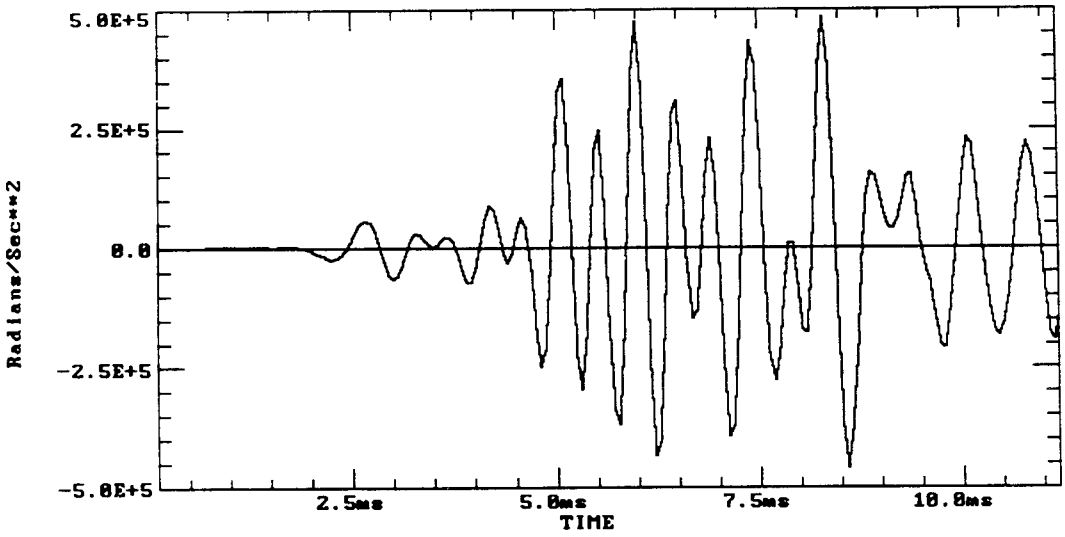

Figure E-14. Case 7 angular acceleration from Task C gun insulator centerline.

INTENTIONALLY LEFT BLANK.

NO. OF COPIES	ORGANIZATION
2	ADMINISTRATOR ATTN DTIC DDA DEFENSE TECHNICAL INFO CTR CAMERON STATION ALEXANDRIA VA 22304-6145
1	DIRECTOR ATTN AMSRL OP SD TA US ARMY RESEARCH LAB 2800 POWDER MILL RD ADELPHI MD 20783-1145
3	DIRECTOR ATTN AMSRL OP SD TL US ARMY RESEARCH LAB 2800 POWDER MILL RD ADELPHI MD 20783-1145
1	DIRECTOR ATTN AMSRL OP SD TP US ARMY RESEARCH LAB 2800 POWDER MILL RD ADELPHI MD 20783-1145
	ABERDEEN PROVING GROUND
5	DIR USARL ATTN AMSRL OP AP L (305)

NO. OF COPIES	ORGANIZATION
1	HQDA SARD TT DR F MILTON WASH DC 20310-0103
1	HQDA SARD TT MR J APPEL WASH DC 20310-0103
11	DIRECTOR ATTN SMCAR CCB C KITCHENS J KEANE T ALLEN J VASILAKIS G FRIAR T SIMKINS V MONTVORI J WRZOCHALSKI G D'ANDREA R HASENBEIN SMCAR CCB R S SOPOK BENET LABORATIES WATERVLIET NY 12189
1	CDR WATERVLIET ARSNL ATTN SMCWV QAE Q C HOWD BLDG 44 WATERVLIET NY 12189-4050
1	CDR WATERVLIET ARSNL ATTN SMCWV SPM T MCCLOSKEY BLDG 25 3 WATERVLIET NY 12189-4050
5	CDR US ARMY ARDEC ATTN SMCAR CCH T S MUSALLI P CHRISTIAN K FEHSAL N KRASNOW R CARR PCTNY ARSNL NJ 07806-5000
1	CDR US ARMY ARDEC ATTN SMCAR CCH V E FENNELL PCTNY ARSNL NJ 07806-5000
1	CDR US ARMY ARDEC ATTN SMCAR CCH J DELORENZO PCTNY ARSNL NJ 07806-5000
1	CDR US ARMY ARDEC ATTN SMCAR CC J HEDDERICH PCTNY ARSNL NJ 07806-5000
1	CDR US ARMY ARDEC ATTN SMCAR CCH P J LUTZ PCTNY ARSNL NJ 07806-5000
3	CDR US ARMY ARDEC ATTN SMCAR TD R PRICE V LINDER T DAVIDSON PCTNY ARSNL NJ 07806-5000
1	CDR PBMA ATTN AMSMC PBM K PCTNY ARSNL NJ 07806-5000
1	CDR USABRDC ATTN STRBE JBC C KOMINOS FORT BELVOIR VA 22060-5606
2	CDR US ARMY MICOM ATTN AMSMI RD W MCCORKLE AMSMI RD ST P DOYLE REDSTONE ARSNL AL 35898
2	CDR US ARMY ARDEC ATTN SMCAR CCL FA H MOORE B SCHLENNER BLDG 65N PCTNY ARSNL NJ 07806-5000
2	CDR US ARMY ARDEC ATTN SMCAR FSA M D DEMELLA F DIORIO PCTNY ARSNL NJ 07806-5000
1	CDR US ARMY ARDEC ATTN SMCAR FSA C SPINELLI PCTNY ARSNL NJ 07806-5000
7	CDR US ARMY ARDEC ATTN SMCAR FSE T GORA E ANDRICOPOULOS B KNUTELSKY A GRAF J BENNETT C DUNHAM R BROGNARA PCTNY ARSNL NJ 07806-5000

NO. OF COPIES	ORGANIZATION
3	PM AFAS ATTN COL NAPOLIELLO LTC A ELLIS G DELCOCO PCTNY ARSNL NJ 07806 5000
1	CDR WATERVLIET ARSNL ATTN SMCWV QA QS K INSCO WATERVLIET NY 12189-4050
2	PM SADARM PCTNY ARSNL NJ 07806-5000
2	PM TMAS ATTN SFAE AR TMA COL HARTLINE C KIMKER PCTNY ARSNL NJ 07806-5000
2	PM TMAS ATTN SFAE AR TMA MD H YUEN J MCGREEN PCTNY ARSNL NJ 07806-5000
2	PM TMAS ATTN SFAE AR TMA MS R JOINSON D GUZIEWICZ PCTNY ARSNL NJ 07806-5000
1	PM TMAS ATTN SFAE AR TMA MP W LANG PCTNY ARSNL NJ 07806-5000
1	DIR USARL ATTN AMSRL CP CA D SNIDER 2800 POWDER MILL ROAD ADELPHI MD 20783
2	PEO ARMAMENTS ATTN SFAE AR PM D ADAMS T MCWILLIAMS PCTNY ARSNL NJ 07806-5000
2	US ARMY RESEARCH OFFICE ATTN ANDREW CROWSON AMXRO MCS J CHANDRA PO BOX 12211 RSRH TRI PK NC 27709-2211

NO. OF COPIES	ORGANIZATION
2	NASA LANGLEY RSRCH CTR MAIL STOP 266 ATTN AMSRL VS W ELBER AMSRL VS S F BARTLETT JR HAMPTON VA 23681-0001
1	CDR ATTN AFWAML R KIM WRIGHT PATTERSON AFB DAYTON OH 45433
2	CDR ARPA ATTN J KELLY B WILCOX 3701 N FAIRFAX DR ARLINGTON VA 22203-1714
6	DIR USARL ATTN AMSRL MA P L JOHNSON B HALPIN T CHOU AMSRL MA PA D GRANVILLE W HASKELL AMSRL MA MA G HAGNAUER ARSNL STREET WATERTOWN MA 02172-0001
1	NAVAL RESEARCH LABORATORY CODE 6383 ATTN I WOLOCK WASH DC 20375-5000
1	OFFICE OF NAVAL RESEARCH MECH DIV CODE 1132SM ATTN YAPA RAJAPAKSE ARLINGTON VA 22217
2	DAVID TAYLOR RESEARCH CENTER ATTN R ROCKWELL W PHYILLAIER BETHESDA MD 20054-5000
1	DAVID TAYLOR RESEARCH CENTER SHIP STRUCTURES AND PROTECTION DEPT ATTN J CORRADO CODE 1702 BETHESDA MD 20084

NO. OF COPIES	ORGANIZATION
4	DIR LLNL ATTN R CHRISTENSEN S DETERESA W FENG F MAGNESS PO BOX 808 LIVERMORE CA 94550
2	BATTELLE PNL ATTN M SMITH M C C BAMPTON PO BOX 999 RICHLAND WA 99352
6	DIR SNL APLD MECH DEPT DIV 8241 ATTN C ROBINSON G BENEDETTI W KAWAHARA K PERANO D DAWSON P NIELAN PO BOX 969 LIVERMORE CA 94550-0096
1	DIR LANL ATTN D RABERN MEE 13 MAIL STOP J 576 PO BOX 1633 LOS ALAMOS NM 87545
1	DREXEL UNIVERSITY ATTN ALBERT SD WANG 32ND AND CHESTNUT STS PHILADELPHIA PA 19104
2	NORTH CAROLINA STATE UNIV CIVIL ENGR DEPT ATTN W RASDORF L SPAINHOUR PO BOX 7908 RALEIGH NC 27696-7908
1	PENNSYLVANIA STATE UNIV ATTN DAVID W JENSEN 223 N HAMMOND UNIVERSITY PARK PA 16802
1	PENNSYLVANIA STATE UNIV ATTN RICHARD MCNITT 227 HAMMOND BLDG UNIVERSITY PARK PA 16802
1	PENNSYLVANIA STATE UNIV ATTN RENATA S ENGEL 245 HAMMOND BUILDING UNIVERSITY PARK PA 16801
1	STANFORD UNIV DEPT OF AERONAUTICS AND AEROBALLISTICS DURANT BUILDING ATTN S TSAI STANFORD CA 94305
1	THE UNIV OF TEXAS AT AUSTIN CTR FOR ELECTROMECHANICS ATTN J PRICE 10100 BURNET ROAD AUSTIN TX 78758-4497
2	VIRGINIA POLYTECHNICAL INSTITUTE AND STATE UNIV DEPT OF ESM ATTN M W HYER K L REIFSNIDER BLACKSURG VA 24061-0219
2	UNIV OF DAYTON RSCH INSTITUTE ATTN R Y KIM A K ROY 300 COLLEGE PARK AVE DAYTON OH 45469-0168
1	UNIV OF DAYTON ATTN J M WHITNEY 300 COLLEGE PARK AVE DAYTON OH 45469-0240
1	PURDUE UNIV SCHOOL OF AERO & ASTRO ATTN C T SUN W LAFAYETTE IN 47907-1282
1	UNIV OF KENTUCKY ATTN L PENN 763 ANDERSON HALL LEXINGTON KY 40506-0046
3	UNIV OF DELAWARE CTR FOR COMPOSITE MATERIALS ATTN J GILLESPE B PIPES M SANTARE 201 SPENCER LABORATORY NEWARK DE 19716

NO. OF COPIES	ORGANIZATION
1	UNIV OF UTAH DEPT OF MECH AND INDUST ENGRNG ATTN S SWANSON SALT LAKE CITY UT 84112
1	UCLA MANE DEPT ENGRNG IV ATTN H T HAN LOS ANGELES CA 90024-1597
1	UNIV OF ILLINOIS AT URBANA CHAMPAIGN NATL CTR FOR COMPOSITE MATLS RSCH 216 TALBOT LABORATORY 104 S WRIGHT ST URBANA IL 61801
1	IAP RESEARCH INC ATTN A CHILLITA 2763 CULVER AVE DAYTON OH 45429
2	FMC CORPORATION ATTN B GOODELL B ANDERSON 4800 EAST RIVER RD MINNEAPOLIS MN 55421-1498
1	ARMTEC DEFENSE PRODUCTS ATTN STEVE DYER 85 901 AVENUE 53 COACHELLA CA 92236
3	ALLIANT TECHSYSTEMS INC ATTN J BODE C CANDLAND K WARD 5901 LINCOLN DR MINNEAPOLIS MN 55346-1674
1	ALLIANT TECHSYSTEMS INC PRECISION ARMAMENTS SYS GRP 7225 NORTHLAND DR BROOKLYN PARK MN 55428
1	CHAMBERLAIN MFG CORP R&D DIV ATTN T LYNCH 550 ESTHER STREET WATERLOO IA 50704

NO. OF COPIES	ORGANIZATION
1	CUSTOM ANALYTICAL ENGRNG SYSTEMS INC ATTN A ALEXANDER STAR ROUTE BOX 4A FLINTSTONE MD 21530
3	IAT ATTN T KIEHNE H FAIR P SULLIVAN 4030 2 W BRAKER LANE AUSTIN TX 78759
1	INTERFEROMETRICS INC ATTN R LARRIVA VP 8150 LEESBURG PIKE VIENNA VA 22100
2	KAMAN SCIENCES CORP ATTN D ELDER T HAYDEN PO BOX 7463 COLORADO SPRINGS CO 80933
3	LORAL VOUGHT SYSTEMS ATTN G JACKSON K COOK L L HADDEN 1701 W MARSHALL DR GRAND PRAIRIE TX 75051
2	OLIN CORP FLINCHBAUGH DIV ATTN E STEINER B STEWART PO BOX 127 RED LION PA 17356
1	OLIN CORP ATTN L WHITMORE 10101 9TH ST NORTH ST PETERSBURG FL 33702
1	DEFENSE NUCLEAR AGENCY ATTN DR R ROHR INNOVATIVE CONCEPTS DIVISION 6801 TELEGRAPH ROAD ALEXANDRIA VA 22310-3398

NO. OF COPIES	ORGANIZATION
1	EXPEDITIONARY WARFARE DIV N85 ATTN DR FRANK SHOUP 2000 NAVY PENTAGON WASHINGTON DC 20350-2000
1	OFFICE OF NAVAL RESEARCH ATTN MR DAVID SIEGEL 351 800 N QUINCY ST ARLINGTON VA 22217-5600
1	NAVAL SURFACE WARFARE CENTER ATTN JOSEPH H FRANCIS CODE G30 DAHLGREN VA 22448
1	NAVAL SURFACE WARFARE CENTER ATTN JOHN FRAYSSE CODE G33 DAHLGREN VA 22448
1	NOESIS INC ATTN ALLEN BOUTZ 1500 WILSON BLVD STE 1224 ARLINGTON VA 22209
1	COMMANDER ATTN DAVID LIESE NAVAL SEA SYSTEMS COMMAND 2531 JEFFERSON DAVIS HWY ARLINGTON VA 22242-5160
1	DEPT OF AEROSPACE ENGNRNG ATTN DR ANTHONY J VIZZINI UNIVERSITY OF MARYLAND COLLEGE PARK MD 20742
1	DEFENSE NUCLEAR AGENCY ATTN LTC JYUJI D HEWITT INNOVATIVE CONCEPTS DIVISION 6801 TELEGRAPH RD ALEXANDRIA VA 22310-3398
1	NAVAL SURFACE WARFARE CTR ATTN MARY E LACY CODE D4 17320 DAHLGREN RD DAHLGREN VA 22448-5000

NO. OF COPIES	ORGANIZATION
	ABERDEEN PROVING GROUND
35	DIR USARL ATTN AMSRL SL BE, CHIEF AMSRL WT WC, CHIEF AMSRL WT WB, W D'AMICO A ZIELINSKI J POWELL AMSRL WT TC, CHIEF R COATES AMSRL WT TA, CHIEF AMSRL-WT-PD, CHIEF W DRYSDALE K BANNISTER T BOGETTI J BENDER R MURRAY R KIRKENDALL T ERLINE D HOPKINS S WILKERSON R KASTE L BURTON J TZENG C JAEGER AMSRL WT PA, CHIEF AMSRL WT PC, CHIEF AMSRL WT PB, CHIEF AMSRL WT PD (ALC), A ABRAHAMIAN K BARNES M BERMAN H DAVISON A FRYDMAN T LI W MCINTOSH E SZYMANSKI H WATKINS

USER EVALUATION SHEET/CHANGE OF ADDRESS

This Laboratory undertakes a continuing effort to improve the quality of the reports it publishes. Your comments/answers to the items/questions below will aid us in our efforts.

1. ARL Report Number ARL-TR-726 Date of Report April 1995

2. Date Report Received _____

3. Does this report satisfy a need? (Comment on purpose, related project, or other area of interest for which the report will be used.) _____

4. Specifically, how is the report being used? (Information source, design data, procedure, source of ideas, etc.) _____

5. Has the information in this report led to any quantitative savings as far as man-hours or dollars saved, operating costs avoided, or efficiencies achieved, etc? If so, please elaborate. _____

6. General Comments. What do you think should be changed to improve future reports? (Indicate changes to organization, technical content, format, etc.) _____

CURRENT ADDRESS

_____
Organization

_____
Name

_____
Street or P.O. Box No.

_____
City, State, Zip Code

7. If indicating a Change of Address or Address Correction, please provide the Current or Correct address above and the Old or Incorrect address below.

OLD ADDRESS

_____
Organization

_____
Name

_____
Street or P.O. Box No.

_____
City, State, Zip Code

(Remove this sheet, fold as indicated, tape closed, and mail.)
(DO NOT STAPLE)

DEPARTMENT OF THE ARMY

OFFICIAL BUSINESS

NO POSTAGE
NECESSARY
IF MAILED
IN THE
UNITED STATES

BUSINESS REPLY MAIL
FIRST CLASS PERMIT NO 0001,APG,MD

POSTAGE WILL BE PAID BY ADDRESSEE

DIRECTOR
U.S. ARMY RESEARCH LABORATORY
ATTN: AMSRL-WT-PD
ABERDEEN PROVING GROUND, MD 21005-5066